

1

Application of Organic Functional Additives in Batteries

1.1 Introduction

Driven by energy transformation and environmental protection, battery technology has received unprecedented attention as key to energy storage and conversion. Lithium-ion batteries (LIBs) are mainly composed of electrolytes, cathodes, and anodes, of which, for liquid electrolytes, separators are often used as supporting materials. As one of the critical materials for battery manufacturing, the electrolyte is mainly used to construct an ion transport channel between cathodes and anodes inside the battery and is a medium for lithium-ion migration and charge transfer (CT) and known as the “blood” of LIBs.

However, with the continuous progress of battery technology, electrolyte performance requirements are also increasing. The traditional electrolyte system has been gradually challenged to meet the needs of modern high-performance batteries, especially in improving energy density, prolonging cycle life, enhancing safety, and other challenges. To address these issues, research on battery electrolyte additives has emerged as a significant area for the advancement of battery science and technology.

Electrolyte additives, as the “fine-tuning agent” in the electrolyte system, can considerably improve the performance of the electrolyte and the battery by introducing a small number of functional additives. Therefore, employing functional additives in the electrolyte is a crucial way to improve the performance of the battery. Additives used in electrolytes need to meet the following primary conditions: (i) soluble in organic electrolytes; (ii) no apparent side effects with other components of the battery; (iii) small dosage and remarkable effect; (iv) no toxicity or negligible toxicity; and (v) low price.

Currently, some widely used additives are fluorinated compounds, nitro compounds, nitrile compounds, phosphate ester compounds, and sulfate ester compounds. This chapter describes the functions of these compounds in batteries in detail and discusses the possible drawbacks of the additives and their solutions.

1.2 Fluorinated Additives

1.2.1 Functions of Fluorinated Additives

1.2.1.1 Improvement of Safety Performance

Fluorinated electrolytes, such as fluoroethylene carbonate (FEC), difluoroethylene carbonate (DFEC), and methyl(2,2,2-trifluoroethyl) carbonate (FEMC), have a relatively lower heat release and a higher onset and peak temperature compared to nonfluorinated carbonates, which results in improved safety performance. Zhang et al. [1] used differential scanning calorimetry (DSC) to evaluate the thermal stability of various commonly used electrolytes and summarized the solvent exothermic phase diagram. The results of the self-extinguishing time (SET) tests have shown that fluorinated electrolytes such as bis(2,2,2-trifluoroethyl) carbonate (TFEC) have better thermal stability as well as flame retardancy. In addition, Meng et al. [2] used fluorinated electrolytes, such as fluoromethyl 1,1,1,3,3,3-hexafluoroisopropyl ether (HFE), to reduce flammability and improve the safety performance of liquid electrolytes.

1.2.1.2 SEI-Forming Additives

Due to the strong electron absorption characteristics of the F functional group, the fluorinated electrolyte's lowest unoccupied molecular orbital (LUMO) is generally lower than that of the ordinary electrolyte, which means that the fluorinated electrolyte will preferentially react with the anode to generate LiF over other solvents [3]. The high surface energy and low diffusion barrier of LiF are conducive to promoting the rapid distribution of Li^+ parallel to the interface to achieve uniform deposition of lithium, which is considered the most favorable inorganic component in the solid electrolyte interface (SEI) [4, 5]. In addition, LiF is a wide-bandgap insulator that prevents electrons from tunneling through the SEI [6]. The formation of dense and uniform inorganic-rich SEI film, on the one hand, can effectively inhibit the further reaction between the anode and the electrolyte [7, 8]. On the other hand, it can improve the reversibility of the anode to form a stable Li^+ plating and stripping process and inhibit the growth of lithium dendrites [9].

Liao et al. [10] observed the presence of LiF in the SEI formed by FEC-added electrolytes using X-ray photoelectron spectroscopy (XPS) and confirmed that FEC with low LUMO has a preferential reduction on lithium metal. In addition to lithium metal anodes, Shin et al. [11] and Li et al. [12] found that FEC on the surface of commercial graphite anodes would also reduce to form a dense, uniform, and LiF-rich SEI, thus enabling a stable graphite–electrolyte interface under low-temperature cycling and conferring excellent cycling stability to the battery. Guo et al. [13] combined classical molecular dynamics (CMD) simulation and XPS analysis of the anode to demonstrate that FEC contributes to the formation of a stable and fluorine-rich SEI and improves the reversibility of Na metal. In addition to the widely studied FEC, fluorinated carbonates such as difluoro-substituted

DFEC [14] and hexafluoro-substituted TFEC [1] are also considered effective solvents for the construction of fluorinated SEIs. The decomposition of DFEC and TFEC can similarly produce the inorganic component LiF to form a dense and homogeneous fluorinated SEI.

The dense SEI formed from the fluorinated electrolyte can inhibit further reactions between the electrolyte and the anode. Nitrile compounds, such as succinonitrile (SN), have been widely used in electrolytes due to the benefits of high ionic conductivity and high oxidation stability, but $-\text{C}\equiv\text{N}$ is highly reactive and easily reacts with lithium metal, so it is quite essential to impede the contact between $-\text{C}\equiv\text{N}$ and lithium metal. The LiF-rich protective layer formed by the degradation of FEC on the surface of lithium metal can effectively inhibit the side reaction between the cyano group and lithium metal, thus improving the cycle performance of the battery [15].

In addition to the decomposition of fluorinated additives to form LiF to change the composition of the SEI, some studies have also shown that the addition of fluorinated electrolytes will change the structure of the SEI. Li et al. [16] observed individual lithium metal atoms and their interfaces with SEI using cryo-electron microscopy and found that the SEI nanostructure formed with FEC was ordered and multilayered: the inner layer was an amorphous polymer matrix, and the outer layer was Li_2O with a large grain size (~ 15 nm). In contrast, the SEI without FEC is a mosaic structure. The authors concluded that the SEI with multilayer nanostructures has better mechanical stability and is more favorable for a homogeneous lithium plating–stripping process. In contrast, the mosaic-structured SEI has poor mechanical properties due to the random distribution of inorganic substances, resulting in possible fracture during cycling and the formation of dead lithium due to the uneven distribution of its grains. In addition, Aurbach et al. [6] suggested that the addition of fluorinated electrolytes, such as FEC, will form a highly cross-linked polymer network on the lithium metal surface, which accommodates the volumetric changes in the contraction and expansion of the lithium metal for lithium deposition and dissolution during cycling.

Based on the outstanding properties of fluoride, some researchers have also used fluoride to modify the lithium metal to improve the performance of the battery. Yan et al. [17] constructed a double-layer film structure, with an outer layer dominated by the organic constituents (ROCO_2Li and ROLi) and an inner layer dominated by the inorganic constituents (LiF and Li_2CO_3) on the Li metal surface through the spontaneous reaction of lithium metal in FEC, as shown in Figure 1.1a. The double-layer membrane structure achieves columnar deposition of lithium by pre-forming uniform deposition nucleation sites. Through the characterization of the morphology of lithium metal after cycling, it is found that the surface of the pretreated lithium metal was smooth and dense, and the lithium deposition was uniform, which inhibited the formation of lithium dendrites. Kim et al. [3] pretreated metal fluoride (M_xF_y) onto lithium metal at a low annealing temperature, and M_xF_y reacted and decomposed with Li to form metallic M nanoparticles and

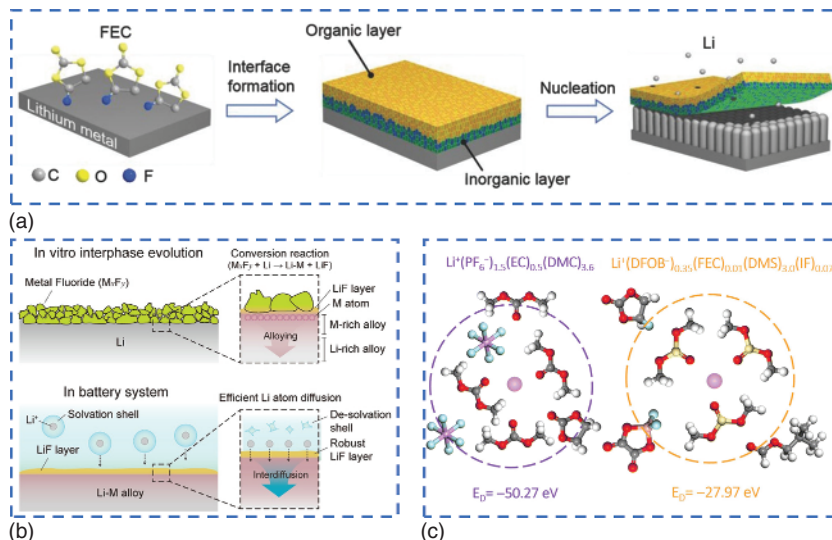


Figure 1.1 Functions of fluorinated additives. (a) The dual-layered film can regulate the uniform deposition of Li ions during repeated charge/discharge cycles and protect the Li metal anode without dendrite formation. Source: Reproduced from Yan et al. [17]/with permission of Wiley-VCH Verlag GmbH & Co. KGaA. (b) Schematic illustration of in vitro interphase evolution employing the conversion reaction of metal fluorides (top) and Li plating/stripping of Li–M alloy with the LiF outermost layer (bottom). Source: Kim et al. [3]/American Chemical Society/CC By NC-ND 4.0. (c) The Li⁺ solvation structures and corresponding desolvation energies of EC + DMC (left) and 45% IF (right) electrolytes. Source: Reproduced from Liu et al. [18]/with permission from Royal Society of Chemistry.

robust LiF inorganic compounds. The metal M nanoparticles formed a uniform Li–M alloy phase with the Li metal, which can promote the formation of a uniform LiF interphase layer and the uniform diffusion of Li, as shown in Figure 1.1b.

However, at the same time, Kim et al. [3] also proposed that the inorganic-rich SEI formed by organic electrolytes with FEC additives on the surface of Li metal is mainly composed of Li₂O rather than LiF and retains an inhomogeneous mosaic-type structure. Tao et al. [19] quantitatively researched the evolution of inactive lithium in lithium-free anode batteries with different electrolytes using mass spectrometry titration and nuclear magnetic resonance (NMR) spectroscopy techniques and found that FEC itself could inhibit the formation of dead lithium metal, but the correlation between LiF formed by the reduction of FEC and dead lithium metal or SEI was weak. Therefore, the assertion that FEC can form a dense and uniform LiF-rich SEI layer needs to be further verified.

1.2.1.3 High Oxidation Stability

Similarly, due to the electron-withdrawing property of the F functional group, the highest occupied molecular orbital (HOMO) of the fluorinated electrolyte is low, indicating high oxidation stability, which can be matched with the high-voltage cathode [20]. Wang et al. [21] proposed a perfluorinated electrolyte FEC/FEMC through potentiostatic testing of graphite||lithium battery and found

that the fluorinated electrolyte showed lower leakage current, which reflects the high-voltage stability of fluorinated electrolyte. The composition and morphology of the cathode electrolyte interface (CEI) layer formed on the recycled graphite revealed that the CEI formed by the fluorinated electrolyte contained less C=O, ROCO_2Li , LiF, and $\text{Li}_x\text{PO}_y\text{F}_z$, suggesting that the reaction between the electrolyte and the graphite cathode was reduced due to the high oxidation stability of the fluorinated electrolyte. It was also observed by transmission electron microscope (TEM) that the fluorinated electrolyte formed a thinner and more uniform CEI.

Although fluorinated electrolytes have relatively low HOMO and are generally challenging to undergo oxidation, some researchers have found that the addition of fluorinated electrolytes may also participate in the formation of CEI. Lu et al. [22] simultaneously introduced 1H,1H,5H-perfluoropentyl 1,1,2,2-tetrafluoroethylether (F-EAE) and FEC into the organic electrolyte of the $\text{LiNi}_{0.5}\text{Mn}_{1.5}\text{O}_4$ (LNMO)-based battery. The electrochemical floatation tests showed that the addition of fluorinated electrolytes significantly reduced the leakage current and improved the oxidation stability of the electrolyte. TEM also revealed that a uniform and thin passivation layer was formed on the surface of the LNMO cathode with the fluorinated electrolyte. The synergistic effect of the two fluorinated electrolytes formed a modification of the cathode, which could prevent the direct contact between the electrolyte and the active cathode particles and further inhibit the dissolution of the transition metal ions. The XPS results showed that the CEI of the fluorinated electrolyte contained a higher content of F and P substances, and the antioxidant capacity was improved, thus increasing the reversible capacity and the cyclic stability performance of the LNMO cathode. Guo et al. [13] found that the CEI formed by the electrolyte with FEC was thinner and denser. It was also found that this CEI was enriched with NaF by XPS, indicating that FEC was also involved in the formation of CEI, thereby protecting the cathode interface. Nagarajan et al. [23] investigated the composition of CEI at different depths by energy-tunable synchrotron-based hard X-ray photoelectron spectroscopy, and it was also found that the addition of FEC to the carbonate electrolyte was also beneficial in improving the film-forming ability of the cathode.

1.2.1.4 Promotion of the Formation of Anion-Rich Solvation Structure

Compared with the widely used carbonate electrolytes and ether electrolytes, fluorinated electrolytes have a weaker solvation ability. Moreover, the stronger electron-withdrawing ability of fluorine atoms can contribute to the distribution of negative charges, lowering the lattice energy of the salt and facilitating the dissolution of lithium salts in the solvent [24]. Su et al. [25] systematically explored the solvation ability of different electrolytes and found that fluorinated electrolytes have lower solvation ability and are less favorable for coordination with Li^+ compared to their nonfluorinated counterparts, but weak solvation can induce more anions to participate in the solvated structure. Zhang et al. [1] compared the solvation ability of ethyl methyl carbonate (EMC), FEC, and TFEC with Li^+ , and the results showed that the binding energy with Li^+ decreased sequentially with the increase of the degree of fluorination, indicating that TFEC is a weakly solvating solvent and rarely

participated in the solvation structure of Li^+ . With the introduction of TFEC, the interaction of Li^+ with the solvent is weakened, but the interaction with the anion is enhanced, again proving that the fluorinated electrolyte can promote the formation of an anion-rich solvation structure. Liu et al. [18] also proposed that the ester-based electrolyte exhibited a weak solvation structure with a low coordination number at low temperatures, and the FEC was free and hardly coordinated with Li^+ , as shown in Figure 1.1c.

In addition, some researchers have suggested that the reason why FEC can decompose to form LiF-rich SEI is also related to the participation in solvation structure. Chen et al. [26] suggested that FEC was selected as the internal solvation complex, thus forming the fluorinated SEI. Su et al. [27] systematically explored the solvation pattern of the SEI-forming agent, FEC, in the electrolyte system and found that the Li^+ was solvated by at least one FEC molecule on average to ensure the formation of stable SEI. If the solvation number of FEC is < 1 , other organic electrolyte molecules coordinated with Li^+ would decompose to form unfavorable SEI. Only when the solvation number of FEC is ≥ 1 , almost all lithium complexes can be preferentially reduced during the formation process to construct fluorinated SEI.

1.2.1.5 Reduction of Desolvation Barrier

The desolvation energy of lithium is also reduced due to the weak solvation of the fluorinated electrolyte. Therefore, the addition of fluorinated electrolytes is expected to reduce the desolvation energy and accelerate the transport kinetics of Li^+ in SEI [28]. Zhang et al. [20] showed that for the electrolyte, from nonfluorinated to perfluorinated electrolyte, the binding energy of solvent molecules to Li^+ decreased, leading to a lower coordination number. The perfluorinated electrolyte optimized the Li^+ -dipole structure and accelerated the desolvation process of solvated Li^+ , which resulted in the generation of SEI with low transport resistance during the plating/stripping process.

1.2.2 Synergies of Fluoroethylene Carbonate with Other Compounds

As the most widely used fluorinated electrolyte, FEC has many advantages. Furthermore, FEC may also have synergistic effects when used with other electrolytes to improve the electrochemical performance of the battery.

1.2.2.1 Fluoroethylene Carbonate and Other Fluorinated Electrolytes

Both FEC and DFEC are fluorinated electrolytes with excellent lithium anode stability. DFEC further reduces the solvation ability of carbonyl oxygen due to the two strong electron-withdrawing fluorine atoms located on both sides of the carbonate [29], so the solvation energy of DFEC is even lower compared to FEC. As DFEC contains two fluorine atoms, its LUMO is also further reduced, which preferentially undergoes reduction on lithium metal over FEC. Aubach et al. [6] found that in high-voltage $\text{Li}||\text{NMC}$ batteries, in the presence of only FEC, the oxidative decomposition products of the electrolyte diffused from the cathode and ultimately to the lithium metal anode, which produced a thicker and more resistive surface

film. However, in the presence of both FEC and DFEC, the DFEC with lower LUMO decomposed and passivated on the Li anode, and then, the FEC acted as a healing agent to continuously “repair” the SEI on the Li anode in the subsequent cycles, which reduced the consumption of FEC.

The bis(trifluoroacetyl)amine (BTFA) molecule has lower LUMO with more fluorine atoms than FEC. Therefore, BTFA will preferentially decompose over FEC to form fluorinated SEI. Wang et al. [30] designed an *in situ* generation of an atomically rooted SEI (R-SEI) based on the synergistic interaction of BTFA and FEC. The results of *ab initio* molecular dynamics (AIMD) simulations showed that in the presence of only FEC, the F atoms generated from the C—F bonds in FEC preferred to stay on the surface of Na (110); in the presence of only BTFA, the F atoms within the molecule were released into the Na interior within 200 fs. However, in the presence of both BTFA and FEC, BTFA induced the F atoms of FEC to enter the inner layer of Na, forming a vertical fluorine concentration gradient. The XPS results showed that the content of inorganic species in R-SEI continued to increase with the sputtering depth, while the content of organic species continued to decrease, suggesting that the solution containing both BTFA and FEC realized a large number of F atoms implanted from the outer layer to the inner layer, forming a multilayer SEI, which was conducive to the improvement of the cycling stability performance of batteries.

1.2.2.2 Fluoroethylene Carbonate and Lewis Base

FEC is a Lewis acid that can accept electron pairs from a Lewis base in the electrolyte environment to form a Lewis acid–base complex. The complex not only can retain its respective functions but also have some synergistic effects. Yang et al. [31] introduced Lewis acid, FEC, and Lewis base, tris(trimethylsilyl) phosphite (TMSP), in carbonate electrolyte, where FEC reacted with TMSP by *in situ* complexation to form a TMSP–FEC complex. TMSP can be used as an impurity scavenger and a CEI-forming additive, while FEC is an SEI-forming additive, and the two synergistically formed an inorganic–organic composite (F/P/Si-rich SEI) and a highly stable CEI. TMSP–FEC complex effectively protected the cathode and the anode and improved the comprehensive performance of the battery, as shown in Figure 1.2.

1.2.2.3 Fluoroethylene Carbonate and Glyme

FEC is thought to reduce to form LiF-rich SEI during the cycling process, but since its structure is similar to that of vinyl carbonate, it is expected to produce some carbon-rich organic substances, such as ROCO_2Li . However, too much carbon-rich organic substance may cover up the LiF-rich SEI formed earlier. As a high donor number (DN) solvent, Glyme has a solubilizing effect on substances rich in C—C—O [32]. Therefore, a certain amount of diethylene glycol dimethyl ether (G2) can dissolve undesired carbon-rich substances on SEI, thereby increasing the content of inorganic compounds in SEI and stabilizing the composition of SEI. Biswal et al. [33] introduced both FEC and G2 into a carbonate-based electrolyte and demonstrated using XPS that the addition of G2 reduced the contents of Li_2CO_3 and C—C—O in SEI, decreasing the activation energy of SEI and CT and increasing the SEI diffusivity and exchange current. In summary, the synergistic effect of FEC and G2 can form

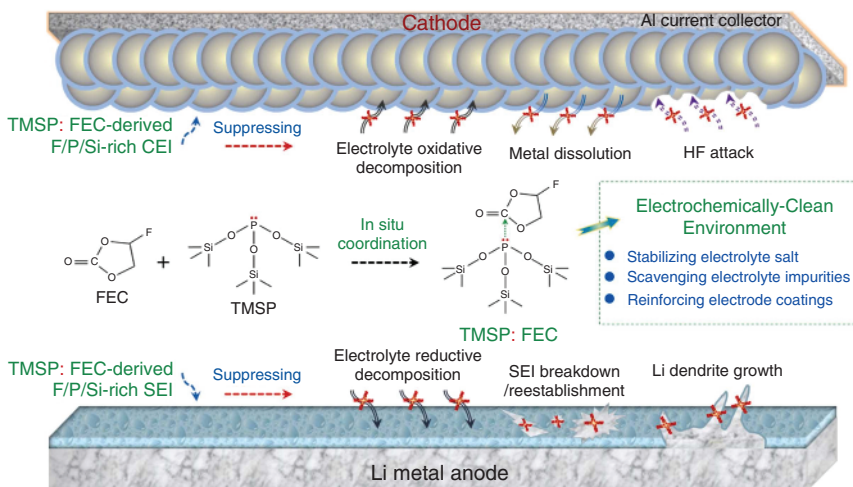


Figure 1.2 Design concept of TMSP–FEC complex as a multifunctional electrolyte additive for lithium metal batteries (LMBs). Source: Reproduced from Yang et al. [31]/with permission of Elsevier.

a stable fluorinated SEI rich in polyene networks, promote the migration of Li^+ in SEI, and facilitate the uniform deposition of Li^+ .

1.2.3 Drawbacks of Fluoroethylene Carbonate

1.2.3.1 Generation of HF Gas

Under the catalysis of Lewis acid PF_6^- or high temperature, FEC is susceptible to dehydrofluorination to produce hydrogen fluoride (HF). On the one hand, the by-product HF will destroy the SEI film, and in the battery with silicon anode, it will corrode silicon particles [34]; on the other hand, HF will lead to the formation of a thicker CEI and catalyze the dissolution of Mn in the case of ternary cathode [11], in addition to corroding the collector aluminum foil [35]. Thus, the generation of HF gas causes irreversible damage to both the anode and cathode, ultimately resulting in a degradation of the cycling performance of the battery.

1.2.3.2 Increase of Impedance and Loss of Impedance

Some researchers have argued that although FEC facilitates the formation of SEI at the anode, it forms a thicker CEI film on the surface of the cathode, which increases the resistance and capacity loss of the battery. Yang et al. [35] found that the initial capacity of $\text{Li}||\text{LiCoO}_2$ (LCO) batteries was significantly reduced after the addition of the FEC additive, which attributed to the excessive decomposition of FEC and resulted in the formation of a thick interfacial layer on the surface of the cathode that hindered the lithium-ion transport.

1.2.3.3 Incompatibility with Other Electrodes

FEC is widely used on lithium metal and silicon anodes, but FEC cannot form stable SEI on graphite anodes. Shen et al. [36] studied the SEI formed on graphite

anodes in different electrolyte systems and found that the SEI formed with the addition of FEC was thicker and denser than that formed with the addition of ethylene carbonate (EC) under the same conditions. Xia et al. [37] investigated the compatibility of FEC-based electrolytes with graphite anodes for the first time. However, the FEC additive was unable to form a protective SEI on the graphite surface because the introduction of F atoms lowered the LUMO of FEC, resulting in a higher reduction potential of FEC than its fluorine-free counterpart EC. However, lithium bis(oxalate)borate (LiBOB) and lithium difluoro(oxalato) borate (LiDFOB), as SEI-forming additives introduced to the electrolyte, could effectively inhibit the reduction of FEC, forming a thin and robust SEI on the graphite anode.

In addition to graphite anodes, for some high-voltage cathodes, FEC may likewise be detrimental to the long-term stable performance of batteries. Aktekin et al. [38] investigated the effect of the FEC additive on LNMO-Li₄Ti₅O₁₂ (LTO) cells. The XPS results indicated that with the increase in the FEC content of the electrolyte, the thickness of the formed CEI increased, and the content of organic substances containing C—C—O also increased, contrary to previous results of the formation of LiF-rich SEI. Cycling and rate performance tests also showed that the addition of FEC did not improve the discharge capacity and the cycling stability of the battery but rather negatively affected the long-term stability of the battery system with a high-voltage LNMO cathode.

1.2.3.4 Recycling Issues

Due to their extreme persistence and challenge in biodegrading, halogenated organic pollutants pose a major threat to human health, the ozone layer, and ecological safety when released into the environment. Fluorine is one of the halogen elements with the most environmental impact among them. Therefore, fluorinated additives are detrimental to the environment in the long run. Consequently, it is imperative to both strictly recycle and dispose the used batteries with fluorinated electrolytes and to design and develop new types of fluorine-free electrolytes that will be more conducive to environmental safety and battery recycling [24].

1.3 Nitro Additive

1.3.1 Functions of Nitro (NO₃⁻)

1.3.1.1 Participation in Solvation and Desolvation Structures

LiNO₃ is a lithium salt with a high DN (22.2 kcal mol⁻¹) [39]. The binding energy of NO₃⁻ to Li⁺ is usually higher than that of conventional lithium salt anions as well as solvent molecules [10]. Therefore, when LiNO₃ is dissolved into the electrolyte, NO₃⁻ is able to expel the solvent molecules from the solvation sheath and preferentially participates in the lithium-ion inner solvation structure, forming an anion-rich solvation environment [40–43]. Zhu et al. [44] confirmed that the addition of NO₃⁻ altered the solvation structure of Li⁺ through Raman spectra, confirming a decrease in the number of both vinylene carbonate (VC) and dimethyl carbonate (DMC) in the

solvation structure, as well as a change in the intensity of the peaks in the infrared spectrum. In addition, Wahyudi et al. [45] found that the addition of NO_3^- shifted the peaks of ^{7}Li NMR toward more positive values, demonstrating the shielding of the electron cloud around Li^+ , indicating a larger solvated cluster scale, as well as the entry of the electron-donating anion, NO_3^- , into the solvation sheath of Li^+ .

Furthermore, NO_3^- enhances the interaction of TFSI^- with Li^+ . In the presence of NO_3^- , the number of free TFSI^- in the electrolyte decreases due to an increase in the number of TFSI^- participating in the Li^+ solvation process. Wahyudi et al. [45] detected the presence of the TFSI^- anion aggregated ion pairs at 747 cm^{-1} in Raman spectroscopy, indicating that NO_3^- enhances the $\text{TFSI}-\text{Li}^+$ interaction. Fu et al. [46] also demonstrated using Fourier transform infrared (FTIR) and Raman spectra that the addition of NO_3^- caused the peaks to be blueshifted, suggesting that TFSI^- existed more in the contact ion-pair (CIP) or aggregated state.

High-concentration electrolyte (HCE) is considered to preferentially compete with solvent molecules due to the increase in salt concentration, forming an anion-rich solvation structure [47]. However, as the salt concentration in HCE increases, the electrolyte becomes more viscous. To improve the overall performance of the electrolyte, diluents such as hydroflurane need to be added to reduce the viscosity to form localized high-concentration electrolytes (LHCEs). However, the aforementioned measures undoubtedly increase the cost of electrolytes [48, 49]. In contrast, the application of NO_3^- additives not only enables NO_3^- itself to participate in the solvation of Li^+ preferentially but also promotes the interaction between TFSI^- and Li^+ , thus achieving an anion-rich solvation environment while ensuring low cost and hardly changing the viscosity of the electrolyte, which is a favorable pathway to realize anion-derived interfacial chemistry.

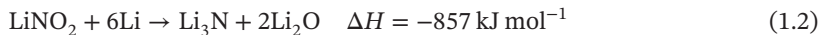
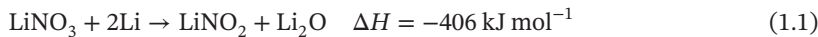
Additionally, NO_3^- not only participates in the formation of solvation structure but also modulates the distance between the Li^+ -solvent-anionic complex and the electrode surface to regulate the properties of the electrolyte and stability of the electrode, thus in turn affecting the thermodynamic and kinetic properties of the Li^+ -solvent-anionic complex during desolvation process at the electrode interface [42]. Anion-rich solvation structures can lower the desolvation energy barrier and promote the Li^+ desolvation behavior [41]. Stuckenbergs et al. [50] demonstrated that higher oxidation currents with LiNO_3 in cyclic voltammetry (CV) tests imply faster kinetics of the lithium electrodeposition/dissolution process, that is, the Li^+ desolvation behavior is effectively enhanced. The additive can change the solvation structure and interface model to promote the desolvation of Li^+ . The “distance” between the Li^+ -solvent-anionic complex and the electrode surface is also a crucial aspect that affects the stability of the electrolyte and electrode.

1.3.1.2 Formation of Inorganic-Rich SEI

Solvation structures are considered to be precursors of SEI, so anion-rich solvation structures have a greater tendency to form anion-derived SEI. However, it is generally believed that the solvent-rich solvation structures are more likely to generate organic-rich SEI, and such organic substances tend to have low ionic conductivity and mechanical properties, which is detrimental to the stability of SEI.

The anion-rich solvation structures are more likely to generate inorganic-rich SEI with superior ionic conductivity and mechanical properties to form a stable SEI [51].

LiNO_3 with low LUMO can preferentially undergo a reduction reaction at the anode over solvent molecules [52]. Reduction reactions tend to go through two processes [53]:



Eight electrons from lithium metal are required for complete decomposition, and the reduction decomposition of NO_3^- anion can lead to more LiN_xO_y components in the anode interface [54, 55]. Ma et al. [52] confirmed the occurrence of the aforementioned reactions by XPS characterization of SEI, where Li_3N , LiN_xO_y , and Li_2O were observed simultaneously, generating inorganic-rich and robust SEI to achieve better protection of lithium electrodes. Thus, an inorganic-rich SEI layer was formed by the reduction decomposition of LiNO_3 with low LUMO. Since NO_3^- enhances the interaction of TFSI^- with Li^+ , more TFSI^- is involved in the solvation structure and ultimately decomposed on the SEI to produce the favorable inorganic component LiF . Zhang et al. [56] found that the content of Li_3N and LiF in the SEI was increased after the introduction of LiNO_3 using XPS, indicating that LiNO_3 may promote the formation of the interface layer rich in $\text{Li}_3\text{N}-\text{LiF}$. It was further verified that the introduction of NO_3^- also promoted the decomposition of TFSI^- . Additionally, the authors simulated the structural configuration changes near the Li anode by AIMD to elucidate the potential mechanism of LiF formation. It was found that the bond lengths of both C—S and C—F bonds were elongated from 0 to 20 ps after the addition of LiNO_3 compared to those without LiNO_3 , which reduced the energy required for bond breaking and accelerated the decomposition of lithium bis(trifluoromethanesulphonyl)imide (LiTFSI). It was demonstrated that LiNO_3 led to the breakage of C—S and C—F bonds of LiTFSI molecules, inducing a large amount of LiF generation in the SEI.

Zhu et al. [44] also succeeded in forming a lithium-indium alloy on the lithium metal anode surface with the introduction of $\text{In}(\text{NO}_3)_3$ additive to change the composition of SEI and improve the electrochemical performance of the battery. Kim et al. [57] introduced both AgNO_3 and LiNO_3 as electrolyte additives to construct SEI with a lithophilic inner layer and a compositionally regulated outer layer on the lithium metal surface sequentially according to their LUMO energy levels. AgNO_3 preferentially deposited on the lithium metal surface to form Ag and Ag_2O due to the lower LUMO energy level (-3.185 eV) to form an inner layer of Ag-based SEI, which significantly reduced the overpotential of the full battery $\text{Li}||\text{NCM}84$.

Due to the high ionic conductivity of the decomposition products of NO_3^- , the transport of Li^+ in SEI and the diffusion kinetics are improved [58]. Inorganic components with high ionic conductivity can effectively reduce lithium nucleation overpotential, leading to larger grain size, which will grow laterally at low density. This growth mode is conducive to reducing the formation of “dead lithium” during lithium plating/stripping, inducing uniform lithium deposition and inhibiting the

growth of lithium dendrites [52, 59, 60]. Liu et al. [61] found that lithium deposition on the Cu surface without LiNO_3 was loose dendrite, while lithium deposition with LiNO_3 was in the form of dense lumps with Li particles growing along the planar direction, indicating that NO_3^- can induce uniform lithium deposition behavior. The inorganic-rich SEI with outstanding ionic conductivity and mechanical strength can reduce the interface impedance, improve the interface contact performance, ensure the stability of the SEI [10, 62], and inhibit the decomposition of solvent molecules [46, 63].

1.3.1.3 CEI-Forming Additives

LiNO_3 can also decompose on the cathode surface to form the CEI to ensure the stability of the cathode and the electrolytes. Fu et al. [46] determined that the addition of LiNO_3 resulted in the appearance of small oxidation peaks at approximately 5.2 V using linear sweep voltammetry (LSV), which corresponded to the decomposition of LiNO_3 . XPS analysis of the CEI showed that the electrolyte with LiNO_3 formed a CEI film with a higher F content compared to the electrolyte without LiNO_3 . In the subsequent static leakage current test, the steady-state oxidative decomposition current of the electrolyte with LiNO_3 was lower than that of the electrolyte without LiNO_3 , which demonstrated that the CEI film with LiNO_3 could inhibit the decomposition of the electrolyte on the cathode surface of the NMC811 and reduce the accumulation of high-resistance decomposition products. The CEI membrane impedance (R_{CEI}) and charge transfer impedance (R_{ct}) of the electrolyte with LiNO_3 were lower, indicating that LiNO_3 accelerated CT kinetics.

Zhu et al. [44] also found that the addition of LiNO_3 altered the components of CEI and inhibited the further decomposition of the subsequent electrolyte using XPS. Fang et al. [41] conducted XPS and TEM to clarify the chemical composition and structure of the CEI layer and observed the presence of LiN_xO_y , a fast lithium-ion conductor, in the CEI layer. Similar to the SEI, the inorganic-rich CEI layer also significantly promoted the interfacial ion diffusion behavior. In addition, only a slight M—O signal was detected in the experimental group with the addition of LiNO_3 , whereas a stronger M—O signal peak appeared in the control group, indicating that the LiNO_3 additive can not only inhibit the decomposition of the electrolyte but also inhibit the dissolution of the transition metal by hindering the vicious reaction between the solvent and the cathode to ensure the structural stability of the cathode.

LiNO_3 also contributes to the stability of the cathode interface through the formation of an electric double layer (EDL). Wen et al. [64] found that NO_3^- exhibited a distinct voltage response effect, that is, it would be enriched at the cathode interface once the cathode was charged, thus forming Li^+ -enriched, thermodynamically favorable EDL with solvent molecules well-coordinated (Figure 1.3). The EDL dramatically accelerated the interfacial reaction kinetics and significantly improved the thermodynamic compatibility between carbonate electrolytes and high-voltage LiTiMnO (LTMO) cathodes.

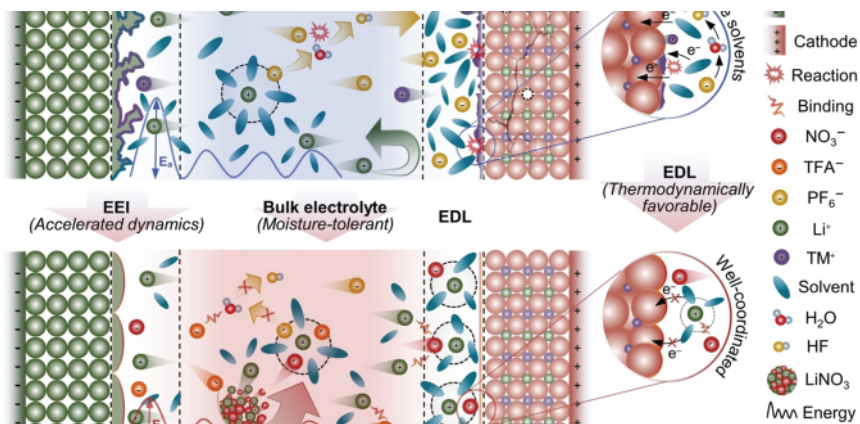


Figure 1.3 Schematic illustration of the reinforced mechanism of the LiTFA–LiNO₃ dual-salt additive on conventional carbonate electrolyte. Source: Reproduced from Wen et al. [64]/with permission of Wiley-VCH Verlag GmbH & Co. KGaA.

1.3.1.4 Functions in Lithium–Sulfur Batteries

NO₃[−] is also an indispensable additive in lithium-sulfur batteries. It was found that LiNO₃ could catalyze the conversion of soluble lithium polysulfide (LiPS) to slightly soluble sulfur as a redox intermediate on the cathode near the end of the charging process (>2.5 V vs. Li/Li⁺), which inhibited the generation and deposition of polysulfide (PS) and prevented it from dissolving into the electrolyte [39, 45, 65]. Meanwhile, LiNO₃ will have a coupling reaction with LiPS to generate a dense passivation layer of LiN_xO_y and LiS_xO_y on the surface of the lithium metal anode, inhibiting the side reaction of LiPS on lithium metal, reducing the formation of dendrites from PS shuttles, and accelerating the redox kinetics [66].

Kim et al. [67] discovered that NO₃[−] can inhibit PS agglomeration through strong coordination with Li⁺. The authors investigated the low-temperature discharge behavior and found that the second discharge plateau of the electrolyte without LiNO₃ disappeared, indicating that the low-order PS formed before the second voltage plateau could not be further reduced to solid Li₂S. The researchers regarded PS aggregation as the conversion block from LiPSs to Li₂S. In contrast, the electrolyte with LiNO₃ showed excellent discharge behavior, and the second voltage plateau of the electrolyte became longer with the increase in LiNO₃ content. It suggests that the electrolyte with a high DN value of LiNO₃ can promote the conversion of LiPS to Li₂S at low temperatures and reduce electrode passivation. Furthermore, the authors demonstrated by density flooding theory (DFT) calculations and molecular dynamics (MD) simulations that anionic NO₃[−] with high DN can inhibit PS agglomeration and promote redox kinetics at low temperatures by strongly coordinating with Li⁺, thus improving the low-temperature performance of the electrolyte.

1.3.1.5 Stabilization of Water Molecules

Zhang et al. [68] found that LiNO_3 can stabilize water molecules through strong hydrogen bonding interactions and inhibit the hydrolysis of PF_6^- anions, thus suppressing the formation of highly corrosive HF. Through MD simulations, the authors discovered strong interactions between H_2O and LiPF_6 , including $\text{O}\cdots\text{Li}^+$ coordination and $\text{O}-\text{H}\cdots\text{F}$ hydrogen bond, which could induce the formation of HF. However, since the solubility of LiNO_3 in water is much higher than that in carbonate solvents, H_2O molecules are surrounded by NO_3^- anions after the introduction of LiNO_3 . DFT calculation results showed that the binding energy of $\text{H}_2\text{O}-\text{LiNO}_3$ (-0.27 eV) was more negative than that of $\text{H}_2\text{O}-\text{LiPF}_6$ (-0.17 eV), which further illustrated that with the introduction of LiNO_3 , H_2O molecules would preferentially coordinate to LiNO_3 , rather than LiPF_6 .

All H atoms in H_2O can form hydrogen bonds with NO_3^- , indicating that NO_3^- anions can effectively stabilize H_2O molecules, thereby preventing the hydrolysis of PF_6^- and the formation of HF. Therefore, LiNO_3 can effectively stabilize the aqueous electrolyte of the lithium metal battery, avoiding the deterioration of battery performance due to the small amount of water molecules in the electrolyte.

1.3.2 Organic Nitro Additive

1.3.2.1 Complex Nitrate-Based Additives

In addition to the basic metal nitrate salts, many researchers have complexed NO_3^- into organic systems. Wang et al. [69] and Hou et al. [54] proposed to link NO_3^- with structural units containing ether functional groups to form an organic nitrate: isosorbide nitrate (ISDN). The solubility of ISDN in the ester-based electrolyte was dramatically increased to 3.3 M due to the high DN value of the ether functional group. Moreover, the combination of ether functional groups broke the chemical resonance inside NO_3^- and enhanced the anti-reducibility of NO_3^- . ISDN can also be decomposed to produce LiN_xO_y -rich SEI, resulting in uniform lithium deposition.

Wang et al. [70] also complexed NO_3^- with oxygen-containing functional groups to develop a novel nitrate-based additive, triethylene glycol dinitrate (TEGDN), to replace LiNO_3 . Unlike LiNO_3 , TEGDN would not interfere with the polymerization of DOL but similarly promoted the formation of a nitrogen-rich SEI layer, which inhibited the parasitic reaction and improved the Coulombic efficiency.

Some other researchers have prepared organic nitrate additives with good solubility in carbonate-based electrolytes by complexing NO_3^- with ionic liquids. Huang et al. [43] combined 1-ethyl-3-methylimidazolium cation [Emim^+] with NO_3^- to develop a novel type of ionic liquid, which facilitated the formation of special Li^+ coordination dissolved structure of NO_3^- , allowing the dissolved NO_3^- to undergo electrochemical reduction and form a stable and conductive SEI. Similarly, Ma et al. [52] complexed 1-methyl-1-decylpyrrolidine cation [Py110^+] with NO_3^- to synthesize an ionic liquid electrolyte additive, which could also be dissolved in the electrolyte without adding a solubilizer. Moreover, NO_3^- could be introduced into the Li^+ solvation sheath of carbonate electrolyte to form an anion-rich solvation

structure. Adiraju et al. [71] combined LiNO_3 with 1-trimethylsilyl imidazole [1-TMSI] groups with similar ionic liquid cationic structures to synthesize a soluble carbonate-based electrolyte additive, TMSILN. The solubility of LiNO_3 was improved by the bonding interaction between 1-TMSI and LiNO_3 . The incorporation of TMSILN improved the rate of performance and reduced the overpotential. Ex situ surface analysis by XPS, FE-SEM, and cryo-TEM showed that thin, uniform SEI containing nitrate reduction products could be generated on lithium metal anode by introducing TMSILN additive to the electrolyte.

1.3.2.2 Complex Nitro-Based Additives

Furthermore, nitro, rather than nitrate, can improve the electrochemical performance of batteries, so some researchers have concentrated their studies on nitro-derived additives. Jiang et al. [72] introduced a nitro-C60 derivative ($\text{C}_60(\text{NO}_2)_6$) as a bifunctional additive into the electrolyte. Nitro-C60 can gather on electrode protuberances via electrostatic interactions and then be reduced to NO_2^- and insoluble C60. Next, the C60 anchors on the uneven groove of the lithium surface, resulting in a homogeneous distribution of Li ions. Finally, NO_2^- anions can react with metallic Li to build a compact and stable SEI with high ion transport. The nitro and C60 acted synergistically to achieve an inorganic-rich SEI as well as a uniform lithium-deposited surface.

1.3.3 Drawbacks and Solutions of Nitro Additives

1.3.3.1 Low Solubility

The most significant drawback of LiNO_3 is its poor solubility ($<10^{-5} \text{ g ml}^{-1}$) in ester-based electrolytes. The DN of conventional ester solvents is smaller than that of NO_3^- ; therefore, the electrostatic interactions between Li^+ and NO_3^- are challenging to break in ester-based electrolytes [73]. The macroscopic result is the difficulty of dissolving LiNO_3 , which dramatically limits its application in the carbonate electrolyte. Many researchers have focused on the solubilization measures of LiNO_3 in ester-based electrolytes, mainly in the following ways:

1) Addition of solubilizers with a high DN value

Introducing solvents with high DN to the electrolyte, such as ethers [74, 75] and sulfolane [46], can effectively improve the solubility of LiNO_3 in the ester-based electrolyte. However, solvents with high DN values tend to have strong solvation ability as well, which may compete with NO_3^- to participate in the solvation structure of Li^+ , thus weakening the solvation effect of NO_3^- . In addition, solvents with high DN values may be incompatible with lithium metal, as well as increase the complexity of operation and experimental cost [44]. Wen et al. [75] introduced tetraethylene glycol dimethyl ether (G4) as a solubilizer of LiNO_3 and proposed a “high-concentration additive” strategy for lithium nitrate. The DN value of G4 is much higher than that of carbonate solvent, and G4 has abundant solvation sites, which can significantly improve the solubility of LiNO_3 .

Meanwhile, ethers have good compatibility with lithium metal, which can avoid violent reactions with lithium metal anode. Even in the presence of G4 with a high DN value, the strategy of “high-concentration additive” ensures that NO_3^- participates in the solvation of Li^+ and forms SEI rich in inorganic substances.

2) Introduction of carrier salts with Lewis acid sites

The electron-deficient Lewis acid can act as an acceptor of electron-rich NO_3^- to decompose LiNO_3 clusters, thereby effectively improving the solubility of nitrate. Some metal ions, such as Al^{3+} , Sn^{2+} , Cu^{2+} , In^{3+} , Ag^+ , Mg^{2+} , and Zn^{2+} , and some weak Lewis acid groups, such as lithium tetrafluoroborate (LiBF_4), have been researched to dissolve LiNO_3 in carbonate electrolyte to form nitrogen-derived SEI. Yan et al. [76] achieved the dissolution of 1.0 wt% LiNO_3 in carbonate electrolytes by adding trace amounts of CuF_2 . LiNO_3 and CuF_2 were added to the electrolyte to achieve simultaneous dissolution, and the blue color of the solution was the result of the action of copper ions. However, due to its involvement in SEI formation, the metal cation may be deposited on the lithium metal anode and separator, posing a risk of short-circuiting [77]. Therefore, the addition of Lewis acid should be considered to promote the formation of robust SEI and dense lithium deposition along with the solubilization of LiNO_3 .

3) Introduction of ions that can coordinate with Li^+ in lithium nitrate

Lewis acid can improve the solubility of LiNO_3 through electron-rich NO_3^- , then the same can be done through the Li^+ of LiNO_3 by introducing groups that can be strongly coordinated with Li^+ to achieve the decomposition of LiNO_3 clusters. Gao et al. [78] and Fang et al. [41] both proposed the introduction of trifluoroacetate anion (TFA^-) to facilitate the dissolution of LiNO_3 in carbonate electrolytes. TFA^- -containing additives are readily soluble in carbonate electrolytes and have better compatibility with lithium metal compared to solvents with high DN. In particular, the carbonyl group ($\text{C}=\text{O}$) of TFA^- can strongly coordinate with Li^+ to promote the dissolution of LiNO_3 , thus optimizing the solvation structure and transport kinetics of Li^+ .

4) Entropy-driven solubilization strategy

Jin et al. [79] correlated the fundamental role of entropy with the limited LiNO_3 solubility and proposed a new low-entropy-penalty design that achieves high intrinsic LiNO_3 solubility in ester solvents by employing multivalent linear esters (Figure 1.4). The authors concluded that the low-polarity DMC molecules would lose a large amount of conformational entropy during the process of binding with Li^+ , forming a transient, unstable solvation structure, which hindered the solubilization of LiNO_3 . However, multivalent linear ester molecules provided multiple ester-group binding sites, effectively reducing the entropy penalty of the coordination process and thus forming a stable solvation structure. In this way, LiNO_3 can directly interact with the primary ester solvents and fundamentally alter the electrolyte properties, resulting in substantial improvements in lithium-metal batteries with high Coulombic efficiency and cycling stability.

Intrinsic: low-entropy-penalty multivalent design

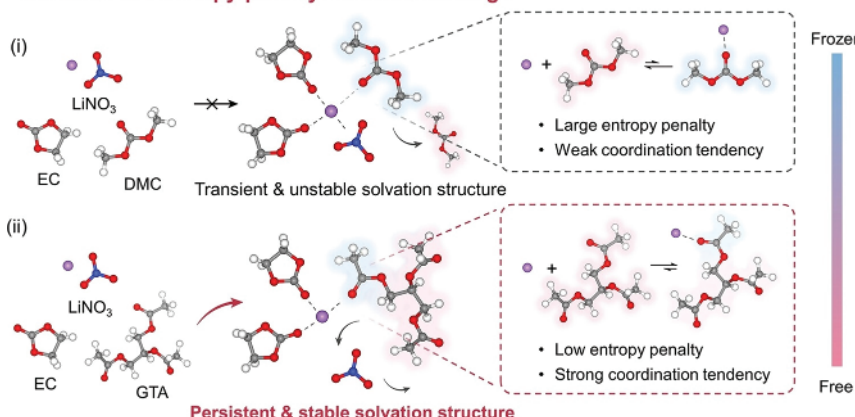


Figure 1.4 Multivalent electrolyte design realizes intrinsic high LiNO_3 solubility due to the low entropy penalty without regulating the enthalpy contribution. Source: Reproduced from Jin et al. [79]/with permission of Wiley-VCH Verlag GmbH & Co. KGaA.

1.3.3.2 Sacrificial Additives

Since the decomposition of NO_3^- during the formation of SEI is irreversible, that is, as the cycling process proceeds, NO_3^- continues to react with the deposited lithium metal until it is exhausted, which is considered a “sacrificial” electrolyte additive. Stuckenbergs et al. [50] prepared LiNO_3 -modified separators by dissolving LiNO_3 in DME and infiltrating it in the separator to load LiNO_3 . The authors found that the LiNO_3 -modified electrolytes showed better cycling stability through cycling tests. Combined with electrochemical tests such as CV, it was concluded that LiNO_3 -modified separators could continuously release LiNO_3 to improve the cycling stability performance of the batteries during the battery cycling process and stabilize its concentration, which effectively overcomes the challenge of depletion of LiNO_3 during the cycling process.

Fu et al. [80] incorporated KNO_3 uniformly into the metal Li anode to prepare the “salt-in-metal” structure Li/KNO_3 (LKNO) composite anode. The concentration change of K^+ in the electrolyte proved that the LKNO electrode stably released KNO_3 into the electrolyte during the cycle to maintain its concentration, avoiding the situation where NO_3^- was depleted and the electrochemical performance deteriorated. The NO_3^- dissolved in the electrolyte effectively improved the performance of the SEI, thereby effectively improving the electrochemical performance of the LKNO composite anode.

In addition, the researcher embedded LiNO_3 powder into metal Li using a simple mechanical kneading method, schematically shown in Figure 1.5a. LiNO_3 and Li metal completely reacted to produce inorganic substances Li_3N and LiN_xO_y , thus realizing the protection of lithium metal [53]. Wang et al. [81] preferentially adsorbed and anchored NO_3^- in LiNO_3 in the anionic vacancy of MgAl layered bimetallic hydroxides (LDHs) through the memory effect, thus achieving the

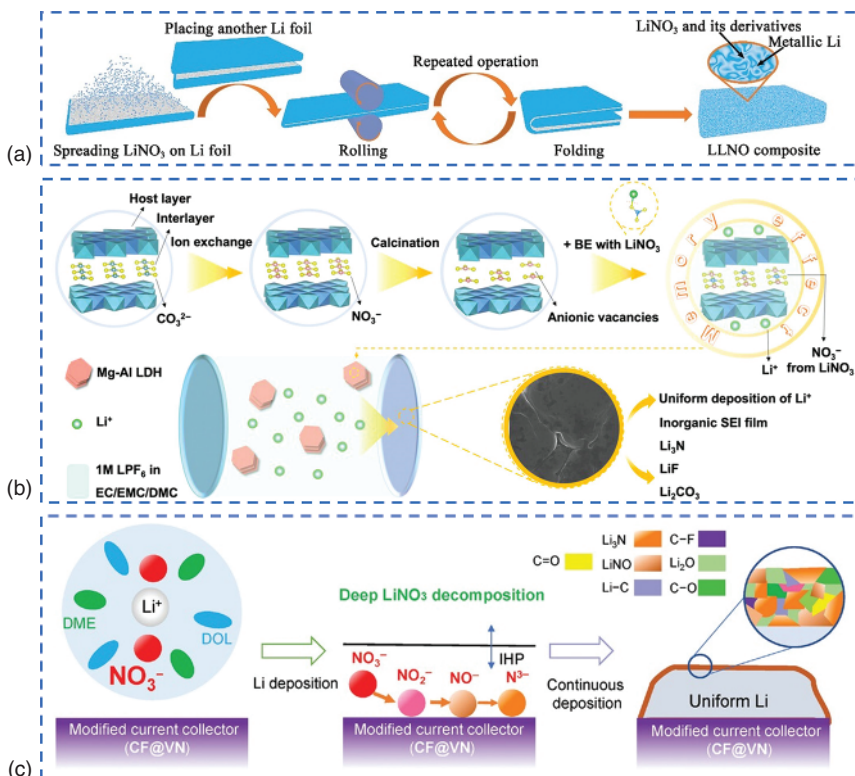


Figure 1.5 Solutions for sacrificial NO_3^- additives. (a) Schematic diagram of the manufacture of Li/LiNO_3 (LLNO) composites. Source: Reproduced from Fu et al. [53]/with permission of Wiley-VCH Verlag GmbH & Co. KGaA. (b) Schematic illustration of designing LDH additive with anionic vacancies for adsorbing NO_3^- anion to promote high dissolution LiNO_3 . Source: Reproduced from Wang et al. [81]/with permission of Wiley-VCH Verlag GmbH & Co. KGaA. (c) The deep decomposition of LiNO_3 on the IHP interface of the catalytic current collector, CF@VN, and schematic representations of the SEI. Source: Reproduced from Zhang et al. [55]/with permission of Wiley-VCH Verlag GmbH & Co. KGaA.

solubilization of LiNO_3 in the carbonate electrolyte and functioning as storing NO_3^- (Figure 1.5b). On the one hand, the reconstituted NO_3^- -MgAl LDHs acted as a sustainable NO_3^- source to avoid the problem of NO_3^- depletion, and on the other hand, the MgAl LDHs could realize the dissolution of LiNO_3 in the carbonate electrolyte, which was conducive to the formation of Li_3N -rich SEIs with high ionic conductivities. The SEI lowered the energy barriers for Li^+ transport, suppressed the growth of lithium dendrites and the side reactions, and formed a uniform and dense Li deposition morphology.

1.3.3.3 High Decomposition Activation Energy of LiNO_3

LiNO_3 reacts with lithium metal during the formation of inorganic-rich SEI and decomposes into inorganic substances with high ionic conductivity and mechanical strength. One LiNO_3 requires eight electrons from the lithium metal

to decompose into one Li_3N and three Li_2O . However, the eight-electron transfer process produces a high energy barrier between LiNO_3 and Li_3N , decreasing the likelihood of the reaction. Zhang et al. [55] showed that lithium oxynitride (LiNO) was identified as a decomposition intermediate, and experimental and simulation results confirmed that LiNO would hinder the further decomposition of LiNO_3 , schematically shown in Figure 1.5c. Therefore, the authors modified the collector, where polar $\text{V}\equiv\text{N}$ bonds were introduced. The study showed that the dipole–dipole interaction between LiNO and the polar $\text{V}\equiv\text{N}$ bond could increase the ionicity of the $\text{N}=\text{O}$ bond and thus reduce its covalency. The decrease in covalency reduces the separation between the bonding and antibonding orbitals, thereby lowering the cleavage energy barrier and promoting the reduction of LiNO_3 to form the inorganic-rich SEI.

1.4 Nitrile Additives

1.4.1 Functions of Nitrile Additives

1.4.1.1 Plasticization

Nitrile compounds are often used as solid polymer electrolytes (SPEs) additives. However, the ionic conductivity of SPEs is generally low. According to the report of Wright et al. [82], the ionic conductivity of fully amorphous polyethylene oxide (PEO) was high, and the activation energy was low, whereas the ionic conductivity of nearly entirely crystalline PEO was rather low at ambient temperature. PEO is a semicrystalline polymer at room temperature, with various forms such as crystal region and amorphous region, and the amorphous region of the activated chain segment is conducive to ion transport. Therefore, lithium ions can only be transported in the amorphous region above the glass transition temperature (T_g). Lithium ions form associations with the active groups on the polymer chain segments, and migration is accomplished by hopping between the chain segments [83].

Therefore, in order to improve the ionic conductivity of polymer electrolytes, some measures will be adopted to destroy the regularity of polymer chain segments to increase the proportion of amorphous regions. Currently, the widely adopted methods are blending, crosslinking, copolymerization, grafting, etc. Among them, adding plasticizer to a polymer matrix is a facile and effective method to improve ionic conductivity. As a micromolecule, nitrile compounds, especially SN, can be introduced into the polymer matrix to reduce the interaction between polymer chain segments to effectively increase the proportion of amorphous region in the polymer matrix, thereby improving the mobility of polymer chain segments and facilitating the migration of Li^+ . Furthermore, nitrile additives may act as chain transfer agents during polymerization, regulating the molecular weight of the polymer, and lower molecular weight means shorter polymer chains, which are more conducive to providing channels for ion migration [84].

Nguyen et al. [85] introduced SN into the polymer electrolyte system of LIBs and found that the addition of SN decreased the crystallization of PEO, and SN had a

synergistic effect with the Nb/Al co-doped $\text{Li}_7\text{La}_3\text{Zr}_2\text{O}_{12}$ (NAL), which contributed to form a uniformly dispersed composite electrolyte and improve the overall performance of the electrolyte. Wang et al. [86] also investigated the plasticization effect of SN on sodium-ion batteries. The addition of SN increased the vibrational energy of the coupling between Na^+ and ether-oxygen in PEO, indicating that the presence of SN weakened the interaction between Na^+ and ether-oxygen, which contributed to the migration of Na^+ through the PEO chain segments and improvement of ionic conductivity. In addition to the PEO matrix, SN was also applied to polymer matrices such as polycarbonate (PC) [87], poly(propylene carbonate) (PPC) [88], poly(vinylidene fluoride-co-hexafluoropropylene) (PVDF-HFP) [89, 90], polyacrylonitrile (PAN) [91], and polyacrylates [92] to improve the ionic conductivity.

1.4.1.2 Facilitation of Ion Transport

Although the introduction of a plasticizer into the polymer matrix can effectively improve the mobility of polymer chain segments, the conduction process of lithium ions in the polymer electrolyte is complicated, and the transport of lithium ions may not only be based on the motility of polymer chain segments but also migrate in the plasticizer-rich microphase. Wang et al. [93] systematically investigated the ionic conduction mechanism of the high ionic conductivity in the SPEs plasticized with SN and found that the addition of SN led to the gradual decoupling of Li^+ from the polymer skeleton and Li^+ recoordinating with SN through ${}^6\text{Li}$ solid-state NMR. The room-temperature ionic conductivity was enhanced significantly by increasing the SN content. When the SN content in the electrolyte reached 50%, the ionic conductivity was comparable to the SN/LiTFSI electrolyte without the polymer, indicating a reduced role of the polymer skeleton in Li^+ conduction. Further experiments revealed that the ionic conduction behavior of SPE shifted from a Vogel–Fulcher–Tammann curve to an Arrhenius curve, suggesting that Li^+ migration occurred mainly through SN rather than the segmental motion of the polymer skeleton. The results indicate that, on the one hand, SN can act as a plasticizer and improve the movement ability of polymer chain segments; on the other hand, when the content of SN is high enough to form a connected phase, the migration mode of Li^+ will change from hopping migration of polymer chain segments to migration in SN-rich microphase.

Liu et al. [84] investigated the transport pathway of Li^+ in SN/polymer matrix and found an interaction between the cyano group ($\text{C}\equiv\text{N}$) and Li^+ in SN and that this coordination may facilitate lithium ion transport by forming the interaction pathway of $\text{C}\equiv\text{N}\cdots\text{Li}^+$. There were three pathways for lithium-ion transport in the electrolyte (Figure 1.6a): (i) $\text{SN} \rightarrow \text{SN} \rightarrow \text{SN}$; (ii) $\text{C}=\text{O} \rightarrow \text{C}=\text{O} \rightarrow \text{C}=\text{O}$; and (iii) $\text{SN} \rightarrow \text{C}=\text{O} \rightarrow \text{SN}$. It suggested that SN could act as a carrier for ionic conduction to improve the ionic conductivity in the SN-rich electrolyte. Hu et al. [94] proposed a Janus quasi-solid-state electrolyte (JSE) design, in which the SN plastic crystal electrolyte was embedded into the Janus host. Through the unique adsorption of SN by LATP, the solvation structures of Li^+ were changed, and a one-dimensional lithium-ion transport channel was constructed inside the solid

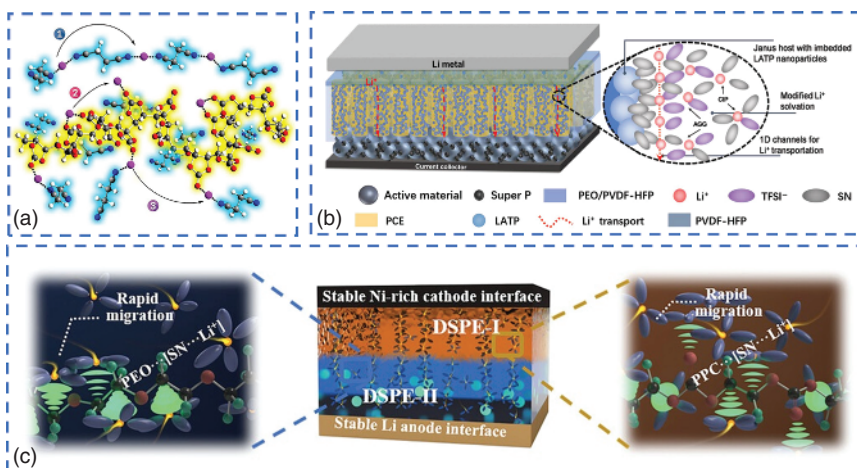


Figure 1.6 Functions of nitrile compounds. (a) Three transference mechanisms of lithium ion in PVCA-SN CPE. The purple balls represent lithium ions. The molecules with blue and yellow light were SN and PVCA, respectively. Source: Liu et al. [84]/John Wiley & Sons/CC BY 4.0. (b) A schematic illustration of the as-designed JSE structure. Source: Reproduced from Hu et al. [94]/with permission of Wiley-VCH Verlag GmbH & Co. KGaA. (c) Structural schematic illustrations of DSPE at room temperature. Source: Reproduced from Wang et al. [88]/with permission of Wiley-VCH Verlag GmbH & Co. KGaA.

electrolyte to enhance the ionic conductivity, as schematically shown in Figure 1.6b. Tong et al. [95] also reported the introduction of SN into $\text{Na}-\text{CO}_2$ batteries by utilizing the room-temperature curing property of SN to construct a layer of highly stable ionic conductive network *in situ* between $\text{Na}_3\text{Zr}_2\text{Si}_2\text{PO}_{12}$ and Ru/ carbon nanotubes (CNT) catalysts. The chemical and electrochemical stability of SN contributed to the extent of the cycling life of solid-state batteries.

In addition to the uniform blending of SN with the polymer matrix, some researchers have separated the SN phase from the polymer matrix, and SN acts as a plastic crystal phase for Li-ion conduction. Lee et al. [92] constructed an elastic solid-state electrolyte with a three-dimensional (3D) interconnected plastic crystal phase by the polymerization-induced phase separation method. The polymer matrix and the plastic crystals within the electrolyte achieved a nanoscale phase separation structure, resulting in the formation of a 3D interconnected network structure of SN phases in the polymer matrix, which provided a fast transport path for lithium ions. Jiang et al. [96] synthesized a composite electrolyte with high ceramic content by solvent-free method. $\text{Li}_{6.75}\text{La}_3\text{Zr}_{1.75}\text{Ta}_{0.25}\text{O}_{12}$ (LLZTO) powder was first bonded with poly(tetrafluoroethylene) (PTFE) and then combined with a nylon mesh framework to form an electrolyte film. The composite electrolyte film was obtained after being immersed in a molten plastic crystal electrolyte (SN/LiTFSI) for 48 hours and by removing excess plastic crystal electrolytes. In this system, the polymer matrix and SN/LiTFSI phase were phase-separated, in which SN no longer acted as a plasticizer but formed a continuous Li^+ transport channel, improving the ion transport efficiency of the electrolyte.

1.4.1.3 Promotion of Lithium Salt Dissolution

Due to the high polarity of the cyano group, compounds containing the $\text{C}\equiv\text{N}$ usually have high dielectric constants, such as SN ($\epsilon = 55$) [97]. Highly polar cyano compounds are able to dissolve various lithium salts up to ≈ 15 mol% [98], thus increasing the concentration of free Li^+ carriers and facilitating rapid ion transport. Wang et al. [88] found that the intermolecular interaction between SN and lithium salt, LiDFOB, can form a specific solvation sheath structure $[\text{SN}\cdots\text{Li}^+]$ through MD simulation. The radial distribution function indicated that the interaction between Li^+ and SN mainly occurred on the N atom, and SN preferentially coordinated with Li^+ , which promoted the dissociation of lithium salt and increased the concentration of Li^+ in the electrolyte. DFT combined with FTIR and NMR results further demonstrated the strong interaction between SN and polymer. Combined with the solvated sheath structure of $[\text{SN}\cdots\text{Li}^+]$, the polymer $\cdots[\text{SN}\cdots\text{Li}^+]$ system constructed a fast lithium-ion transport channel, providing a driving force for the transport of lithium ions through the polymer chain segment at room temperature, as schematically shown in Figure 1.6c.

1.4.1.4 Widening of the Electrochemical Window

The cyano groups with low HOMO endow nitrile compounds with high oxidation stability. Therefore, the addition of nitrile compounds to the electrolyte can broaden the electrochemical window of the electrolyte [89], which in turn meets the requirements of matching the high-voltage cathode and expands its application range in LIBs [84]. Zhang et al. [99] found that compared with pure polyethylene glycol methyl ether acrylate (PEGMEA)-based electrolytes, electrolytes with SN showed a wider electrochemical stability window, up to 4.8 V, which met the application requirements of the high-voltage cathode.

1.4.1.5 Inhibiting the Decomposition of the Electrolyte

Researchers have found that the cyano group can also coordinate with transition metal ions on cathodes, thus changing the charge density of the metal ions, lowering their oxidation states, and inhibiting their catalytic decomposition of the electrolyte. Yang et al. [35] explored the mechanism of nitrile compounds on the surface of the LCO cathode by combining Vienna ab initio simulation package calculations and soft X-ray absorption spectroscopy. The results revealed that $-\text{CN}$ inhibited the catalytic decomposition of transition metal ions in the LCO cathode to the electrolyte during the charging process. It was observed by TEM that the CEI formed by the electrolyte of 10% FEC without nitrile additives was of high thickness and non-uniform, while the CEI formed with 1% suberonitrile or 1% 1,3,6-hexantrionitrile (HTCN) was dense, thin, and electrically insulated. The thin CEI indicated that the excessive decomposition of FEC on the surface of the cathode was suppressed by nitrile compounds, improving the high voltage stability of the LCO cathode.

1.4.1.6 Low Flammability

SN, as a representative of nitrile additives, is nonflammable and nonvolatile, which has been reported in many articles [96, 100, 101]. The plastic crystals of nonflammable nitrile additives, combined with the polymer matrix with non-leakage

properties. The polymer matrix can further enhance the safety of the electrolyte and avoid the risk of thermal runaway at high temperatures [102]. Wang et al. [88] conducted ignition tests on SPE containing SN and found that it was difficult to ignite and only melted gradually even after 90 seconds of flame contact, suggesting that the electrolyte had excellent fire protection potential. Jiang et al. [96] also conducted combustion experiments on a celgard separator and PTFE-LLZTO-SN electrolyte. The separator rapidly shrunk and burned close to the ignition source, whereas the PTFE-LLZTO-SN electrolyte exhibited excellent nonflammability due to the low flammability of SN and the excellent thermal stability of the PTFE-LLZTO framework. Therefore, the nonflammable PTFE-LLZTO-SN electrolyte could eliminate the risk of thermal runaway and effectively improve the safety performance of lithium batteries.

1.4.1.7 Improvement of Polymer Flexibility

SN-based electrolytes turn into a liquid state when heated to their melting point and return to solid state upon cooling, the property that helps to maintain the compactness and flexibility of the composite electrolyte [96]. The addition of an appropriate amount of SN to the electrolyte can improve the elasticity and plasticity of the polymer electrolyte film [86]. Lee et al. [92] proposed that SN, as a plastic crystal, enhanced the mechanical elasticity of the material, enabling the electrolyte to accommodate volume changes during the charge and discharge of lithium metal, thus improving the cycle stability of the battery.

1.4.1.8 Modification of the Cathode Interface

Due to the high oxidative stability of nitrile compounds, nitrile compounds tend to match well with the cathode. Therefore, some researchers have introduced nitrile compounds as functional additives into the electrolyte to stabilize the cathode. Lee et al. [103] introduced adiponitrile (AN) into liquid electrolytes, as a novel bifunctional additive. XPS results showed that the cyano group could affect the oxidation state of the cathode surface, form a strong coordination with Ni^{4+} of the cathode, and inhibit the formation of unfavorable Ni^{2+} . Detrimental Ni^{2+} usually forms an irreversible NiO -type rock salt structure on the cathode surface. Therefore, the addition of AN could effectively inhibit the side reaction on the cathode surface and improve the interfacial stability of the nickel-rich NCM cathode surface.

Moreover, nitrile compounds can also be used as an electrolyte modification layer and compounded into the electrolyte with poor cathode matching to form a multilayer electrolyte film. Chen et al. [104] modified the plastic-crystalline electrolyte (PCE) layer containing SN onto the LLZTO (LLZTO-PCE) surface to reduce the interface impedance between the solid-state oxide electrolyte, LLZTO, and the cathode. PCE film with high ionic conductivity ($7.2 \times 10^{-4} \text{ S cm}^{-1}$) could maintain excellent ionic conduction characteristics and maintain the stability of the interface with the cathode. Liu et al. [105] reported a durable $\text{Li}_{1.5}\text{Al}_{0.5}\text{Ge}_{1.5}\text{P}_3\text{O}_{12}$ (LAGP)-based Li metal battery by employing self-healing polymer electrolytes (SHEs) as Janus interfaces. The SHEs were constructed on both sides of LAGP pellets by in situ polymerization of a functional monomer and a cross-linker in

ionic liquid-based (anodic side in contact with Li metal) or AN-based cathodic gel polymer electrolyte (CGPE). The as-developed SHEs show flame-retardant, high ionic conductivity ($> 10^{-3}$ S cm $^{-1}$ at 25 °C), excellent interfacial compatibility with electrodes, and effective inhibition of Li dendrite formation. AN-based CGPE was prepared by polymerizing 1.5 wt% PETEA monomer into 1 M LiTFSI in AN cathode liquid electrolyte (CLE). AN is chosen for cathodic side electrolytes due to its high oxidation stability and ionic conductivity.

1.4.1.9 Involvement in the Solvation Structure of Zn²⁺

Nitrile compounds also play an essential role in aqueous zinc-ion batteries. During the electrochemical deposition of zinc metal batteries, there is a problem in the decomposition of water molecules into hydrogen due to proton reduction, and current research efforts are devoted to changing the solvation structure of Zn²⁺ to inhibit the dehydrogenation reaction. It has been found that some nitrile compounds, such as SN or acetonitrile, can coordinate with metal zinc ions, thus inhibiting water molecules from participating in the solvation of Zn²⁺ and changing the solvation structure of conventional hydrated zinc ions to restrain the generation of hydrogen [106]. In addition, Yang et al. [107] found that the coordination of SN with Zn²⁺ inhibited the interaction between Zn²⁺ and water molecules and promoted the uniform deposition of metal zinc on the anode, forming a highly uniform Zn deposition with mosaic morphology. The lack of free water in the solvation structure of Zn²⁺ on the cathode inhibited the dissolution of poly(2,3-dithiino-1,4-benzoquinone) cathode.

1.4.1.10 Weakening of Ionic Association

For the graphite cathode in the dual-ion batteries (DIBs), the severe ion association behavior will cause the anions on the cathode surface to be bound by the multivalent metal cation during the charging process, and the coinsertion of metal cations will occur when the anion is inserted into the cathode. The large size of intercalated anionic complexes leads to a significant decrease in the number of sites practically viable for capacity contribution inside graphite galleries in the energetically favorable single-stacking mode, compromising the intrinsic capacity of graphite cathodes for anion storage. Yang et al. [108] found that the addition of high dielectric constant AN as a cosolvent in the electrolyte could weaken the ion association and inhibit the cation co-insertion behavior, significantly improving the specific capacity of graphite cathode.

1.4.1.11 Contribution to the Formation of SEI

Generally, nitrile compounds with high LUMO will not contribute to the formation of SEI. However, Song et al. [109] found the dipole–dipole interactions between the locally negatively charged N atoms in $-\text{C}\equiv\text{N}$ of SN and the locally positively charged C atoms in $-\text{O}-\text{C}=\text{O}$ of PMMA. The interactions induced $-\text{C}\equiv\text{N}$ to be reduced to Li₃N in the SEI layer, forming a stable SEI layer, which facilitates a uniform lithium deposition and better interfacial stability of lithium metal batteries during cycling.

1.4.2 Compatibility Analysis of Nitrile and Lithium Metal

1.4.2.1 Incompatibility of Nitrile and Lithium Metal

The most critical issue limiting the wide application of nitrile compounds in LMBs is the incompatibility of the cyano group in contact with the lithium metal anode. Lin et al. [9] investigated the mechanism of the degradation of the lithium metal anode with SN-based SPE. Due to the lack of a stable SEI between the lithium metal and the SPE, there was a sustained spontaneous reaction between the lithium metal, SN, and the polyacrylate polymer skeleton, generating large amounts of Li_xNC as decomposition products. Some studies suggest that the SN-based PCE will be catalyzed by lithium metal to undergo nitrile polymerization, which will lead to the interface incompatibility between the anode and the electrolyte and reduce the stability of LMBs [89].

1.4.2.2 Improvement of the Compatibility of Nitrile and Lithium Metal

Currently, the typical solutions for the aforementioned problems mainly include the formation of a stable SEI layer, a decrease in the reduction activity of the cyano group, restriction of the migration of nitrile additives, and in situ formation of a lithium metal protective layer.

1) Formation of a stable SEI layer

As mentioned earlier, an essential function of fluorinated additives is the SEI-forming agent, so a certain amount of FEC can be added to the electrolyte. FEC can preferentially form an inorganic-rich SEI layer on the surface of lithium metal to effectively inhibit the contact between the cyano group and lithium metal and avoid side reactions [9]. Alternatively, the lithium metal anode is pretreated to form a Li-FEC anode. The Li-FEC anode with a LiF-rich protective layer can prevent the reaction between the lithium anode and the plastic crystal components in the electrolyte, thus improving interfacial compatibility. The surface of the Li-FEC anode was relatively flat after cycling without the presence of by-products and dendrites, which successfully verified that the designed FEC-optimized lithium anode possessed good compatibility with the electrolyte-containing SN [96].

Dual-salt strategy can also effectively improve the compatibility between SN and lithium metal [15, 110, 111]. Bao et al. [89] introduced a dual salt strategy of LiTFSI and LiBOB to investigate the incompatibility between SN and Li metal. Through SEM and FTIR tests, it was proved that the addition of LiBOB could effectively inhibit the polymerization of SN, catalyzed by Li metal. XPS analysis showed that, compared with the formation of SEI formed by LiTFSI alone, the B—F bond signals were observed on the surface of lithium metal with double salts (Figure 1.7a), indicating the involvement of LiBOB in the formation of SEI. Moreover, it was hypothesized that LiBOB assisted in the formation of the SEI film, thereby inhibiting the harmful side reactions of SN with Li metal.

2) Decrease in reduction activity of cyano group

The reason why nitrile compounds react adversely with lithium metal is that the reduction activity of the cyano group is too high. The poor reduction stability

of the electrolyte will further lead to the decomposition of the electrolyte near the lithium metal anode, resulting in irreversible stripping/plating of lithium and, ultimately, battery failure [113]. Therefore, we can chemically reduce its reduction activity and thus inhibit the reaction between cyano groups and lithium metal. Zhang et al. [101] experimentally and theoretically confirmed the existence of strong electrostatic interactions between α -hydrogen in SN and oxygen-rich ether in 1,3,5-trioxane (TEX) (Figure 1.7b). Intermolecular CT between SN and TEX decreased the reduction activity of SN and increased steric hindrance, both of which together inhibited the side reaction of SN with lithium metal and improved the reduction stability of the electrolyte. Zhang et al. [114] proposed the introduction of the LLZTO, which utilized the La^{3+} in LLZTO to coordinate with the $-\text{C}\equiv\text{N}$ of the SN, thereby increasing the electron density of the cyano group, leading to the polymerization of the SN, which in turn reduces the reactive $-\text{CN}$ groups or converts them to less reactive $-\text{C}=\text{N}-$ groups, thus inhibiting the reaction of SN with lithium metal. However, the polymerization of SN will sacrifice the ionic conductivity of the electrolyte. Therefore, better methods can be adopted instead of the polymerization of cyano groups.

3) Restriction of the migration of nitrile additives

Nitrile additives, like SN, migrate in the electrolyte into an anode and thus react with Li metal. However, the contact of nitrile compounds with Li metal can be avoided by constructing a hierarchical solid-state electrolyte (HSE), where nitrile compounds are kept away from the Li metal side, and their migration is limited. Fu et al. [100] designed an HSE structure, in which SN-based quasi-solid electrolyte (sIQSE) was matched with NCM622 cathode, and PEO-based polymer solid electrolyte (oPSE) was matched with lithium metal anode. The SN-based antioxidation layer was in contact with the high-voltage cathode, and the PEO-based antireduction layer was in contact with the lithium anode, as schematically shown in Figure 1.7c. However, the layered electrolyte structure was insufficient to restrict the movement of SN, and SN can still diffuse freely through the interface between sIQSE and oPSE, and reach the surface of the lithium anode during cycling. Therefore, it was necessary to further introduce substances that could restrict the migration of SN, and nano LLZTO was thus introduced into sIQSE. By utilizing the complexation between the La atoms in LLZTO and the N atoms in SN, the free SN molecules were successfully immobilized in the SN-based electrolyte layer, which prevented free SN from diffusing to the lithium anode side and ensured the stability of lithium metal.

Similarly, Wang et al. [88] proposed a heterogeneous bilayer solid-state polymer electrolyte (DSPE) with a structure divided into SN-PPC-LiDFOB (DSPE-I) compatible with the cathode and PEO- $\text{Li}_7\text{La}_3\text{Zr}_2\text{O}_{12}$ -LiTFSI (DSPE-II) compatible with the lithium anode. Unlike the previous work, LLZO was added into the electrolyte on the anode side, while the limitation of SN relied on the polymer matrix PPC on the cathode side. According to the calculation of electrostatic potential (ESP), the coordination between polymer matrix PPC and SN in DSPE-I was stronger than that of PEO in DSPE-II, that is, SN was more inclined to stay in DSPE-I near the cathode, thus limiting the contact between SN and lithium metal. Zhang et al. [99] also proposed that due to the interaction between

SN and the polymer matrix PEGMEA within the electrolyte, the migration of SN was limited, which enhanced the stability of the interface between SN and the lithium metal anode.

4) In situ formation of a lithium metal protective layer

In addition to the artificial construction of layered solid-state electrolytes, a protective layer can also be in situ constructed on the surface of lithium metal from the composition of the electrolyte. It is worth noting that the protective layer here is different from SEIs, whereas SEIs with excellent performance tend to be membranes dominated by inorganic compounds with certain functions such as rapid Li^+ conduction and uniform Li^+ deposition, and the protective layer here focuses more on protecting the Li metal from reacting with SN. Wu et al. [112] found through DFT calculation that LiDFOB with low LUMO energy would preferentially reduce to BF_3 on lithium metal, and BF_3 would further induce TXE in situ polymerization to polyformaldehyde (POM) on the surface of lithium metal (Figure 1.7d). Further calculations revealed that compared to SN, POM would preferentially adhere to the lithium metal surface. POM with a stable LUMO energy level was compatible with Li metal, effectively inhibiting the contact between SN and lithium metal. Liu et al. [84] found that VC would also react on the surface of lithium metal preferentially to SN to form a protective layer in the VC-SN-LiDFOB system, which prevented the direct contact between SN and lithium metal and effectively improved the interface between electrolyte and lithium metal.

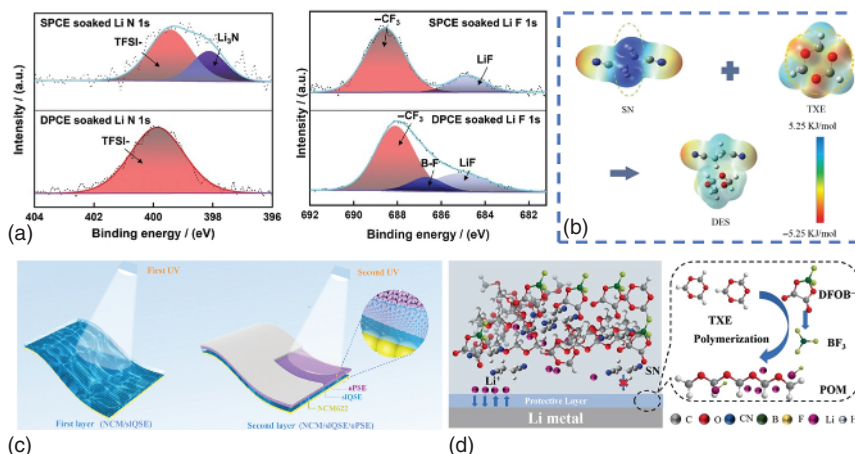


Figure 1.7 Solutions to improve the compatibility of nitrile compounds with lithium metal. (a) XPS profiles of SPCE-soaked Li (top) and DPCE-soaked Li (bottom). Source: Reproduced from Bao et al. [89]/with permission of Wiley-VCH Verlag GmbH & Co. KGaA. (b) ESPs map of total electron density for SN, TXE, and DES. Source: Reproduced from Zhang et al. [101]/with permission of Wiley-VCH Verlag GmbH & Co. KGaA. (c) Schematic representation of the detailed synthesis process and the assembly process of HSE/cathode composite. Source: Reproduced from Fu et al. [100]/with permission of Wiley-VCH Verlag GmbH & Co. KGaA. (d) The formation mechanism of a protective layer on the surface of Li metal. Source: Wu et al. [112]/John Wiley & Sons/CC BY 4.0.

1.4.3 Other Drawbacks of Nitrile Additives

1.4.3.1 Low Mechanical Strength

SN, as a typical nitrile compound, is solid-state at room temperature, but when complexed with lithium salts to prepare PCEs, SN-based PCEs exhibit low melting points and transform into viscous liquid electrolytes [109]. PCEs are insufficient for the formation of self-supporting electrolyte membranes without complexing with a polymer matrix. Self-supporting electrolytes can be achieved by incorporating SN into the polymer network to construct poly(plastic-crystalline electrolytes) (PPCEs) [115]. If nitrile compounds are introduced into polymer-based electrolytes as plasticizers, although the degree of polymerization of the electrolyte will be reduced to improve the ionic conductivity, the mechanical properties of the electrolyte will be decreased as well. Therefore, in the regulation of the ratio of electrolyte to plasticizer, we should pay attention to the balance between ionic conductivity and mechanical properties.

1.4.3.2 Prone to Polymerization

As mentioned earlier, there is a strong coordination between the La^{3+} in LLZTO and the cyano group in SN, which leads to the polymerization of SN. Although the polymerization of SN can inhibit the reaction between the cyano group and lithium metal, the ionic conductivity of the electrolyte system will decrease. Yang et al. [116] induced coordination competition by introducing a strongly polar PAN polymer matrix into the system. There was also a strong interaction between SN and PAN, which weakened the coordination between SN and La^{3+} , thus inhibiting the polymerization of SN. Therefore, the prepared PAN-modified SN electrolyte exhibited a stable and high ionic conductivity ($10^{-4} \text{ S cm}^{-1}$).

1.4.3.3 Crystallinity

The crystallinity of SN molecules affects the ionic conductivity, especially at low temperatures, and the increase in crystallinity and viscosity of the molecules will weaken the ionic conductivity of the electrolyte. Kim et al. [115] investigated the effect of the polymer network on the morphology of SN in PPCEs, exploring the binding energies between SN and polymer units by dispersion-corrected density functional theory (DFT-D) simulations. It was found that miscibility determined the conformation and crystallization behavior of SN in polymer networks. The variation of the binding energies between SN and polymer units significantly affected the formation of amorphous phases in PPCEs. Polymer units with high binding energies [e.g. vinyl ethylene carbonate (VEC)] could hinder the aggregation of SN, promote the formation of the amorphous phase, and improve ionic conductivity. These findings highlighted the importance of optimizing the miscibility of components in PPCE to achieve amorphous phases, thus facilitating efficient ion transport. Wang et al. [102] found that through interaction with ethoxylated trimethylpropane triacrylate (ETPTA), crystallization of SN was inhibited, ensuring proper ion migration over a wide temperature range.

1.5 Phosphate Ester Additives

1.5.1 Functions of Phosphate Ester Additives

1.5.1.1 Flame Retardant

Safety is one of the most severe challenges in commercial carbonate electrolytes. Carbonate electrolytes are often flammable. They will cause fires, explosions, and other major safety issues, so the development of electrolytes with flame-retardant properties is an urgent problem to be solved currently. According to the free radical mechanism of combustion, the flame retardant of the electrolyte can be carried out from two aspects: on the one hand, it can reduce the ability of the electrolyte to generate free radicals, such as the use of nonflash point, high flash point, low melting point or nonvolatile solvents; on the other hand, it can introduce flame retardant to improve the ability of the electrolyte to clear free radicals [117].

Phosphate ester additives are one of the most widely used flame retardants in electrolytes. Phosphate ester additives will decompose when heated, forming phosphorus free radicals ($\text{PO}\bullet$), which can remove combustion free radicals ($\text{H}\bullet$, O_2^* , $\text{HO}\bullet$), thus blocking the combustion chain reaction [118]. Therefore, the addition of phosphate ester into electrolytes will reduce the exothermic value and self-heating rate of batteries and improve the thermal stability of the electrolytes. Currently, widely researched phosphate flame-retardant additives for LIBs mainly include trimethyl phosphate (TMP) [119, 120], triethyl phosphate (TEP) [121, 122], dimethyl methylphosphonate (DMMP) [123], diethyl ethyl phosphate (DEEP) [124], etc.

TMP is a kind of phosphate ester flame retardant with the simplest structure. Wang et al. [125] described the flame-retardant mechanism of TMP, which could be divided into three parts: (i) gasification of TMP under heat: $\text{TMP}_{\text{liquid}} \rightarrow \text{TMP}_{\text{gas}}$; (ii) decomposition of gaseous TMP in flame to produce phosphorus-free radicals: $\text{TMP}_{\text{gas}} \rightarrow [\text{P}]\bullet$; (iii) elimination of hydrogen radicals that sustained the combustion chain reaction by phosphorus-free radicals: $[\text{P}]\bullet + \text{H}\bullet \rightarrow [\text{P}]\text{H}$. The combustion chain reaction was interrupted by the lack of hydrogen radicals. The structure of TEP is similar to TMP, and Li et al. [126] used TEP as a flame-retardant electrolyte, which exhibited a low SET of 6.10 s g^{-1} , while the SET of 1 M LiPF_6 EC/DEC in the conventional carbonate system was as high as 48.92 s g^{-1} . SET is the duration for which the electrolyte continues to burn after the external fire source is removed. Generally, if the SET of the electrolyte is $< 6 \text{ s g}^{-1}$, it is “nonflammable”; $6 \text{ s g}^{-1} < \text{SET} < 20 \text{ s g}^{-1}$ is “flame retardant”; $> 20 \text{ s g}^{-1}$, it is “flammable.” It could be seen that the electrolyte of the phosphate ester system had excellent flame retardant.

Fluorinated phosphate esters are also widely studied functional additives, such as tris(hexafluoroisopropyl)phosphate (THFP) [127], pentafluorophenyl diethoxyphosphate (FPOP) [118], and tris(2,2,2-trifluoroethoxy) phosphate (TFP) [128]. Gu et al. [128] prepared the electrolyte by mixing TFP with γ -butyrolactone (GBL) solvent, using LiPF_6 as lithium salt and adding lithium difluoro(oxalato)borate (LiODFB) as a film-forming additive to improve the

interface stability of the electrode. The combustion experiments found that the conventional commercial electrolyte 1 M LiPF₆ in EC/DMC was ignited at the instant of contact with the fire source and continued to burn for 110 s. After adding 30 wt% TFP flame retardant, the electrolyte could still be ignited but only lasted for 6 s, indicating that TFP had outstanding flame-retardant performance. However, when the solvent was replaced by GBL and TFP (the mass ratio of the two was 70 : 30), the electrolyte could not be ignited. This indicates that GBL is less flammable than the conventional electrolyte EC/DMC. Combined employment of GBL and TEP provides superior nonflammable performance for the electrolyte, significantly enhancing the safety performance of batteries.

1.5.1.2 Stabilization of Cathodes and Anodes

TMSP, as a typical phosphate ester, is also a widely used electrolyte additive, which is able to passivate the metal oxides of the cathode and form a stable CEI layer [129]. The CEI can reduce the polarization voltage of the charging and discharging process so that the battery can still maintain good cycling and rate performance during the cycling. Zhao et al. [130] proposed an *in situ* “anchoring + pouring” synergistic CEI construction (Figure 1.8a), realized by using HTCN and TMSP electrolyte additives. HTCN with three nitrile groups could tightly anchor transition metals by coordinative interaction to form the CEI framework, and TMSP would electrochemically decompose to reshape the CEI layer. The uniform and robust *in situ* constructed CEI layer could suppress the transition metal dissolution, shield the cathode against diverse side reactions, and significantly improve the overall electrochemical performance of the cathode.

However, regarding the stabilizing effect of TMSP on the cathode, some researchers propose that TMSP is not directly involved in the formation of CEI. Liao et al. [133] introduced TMSP into the electrolyte and found that the morphology

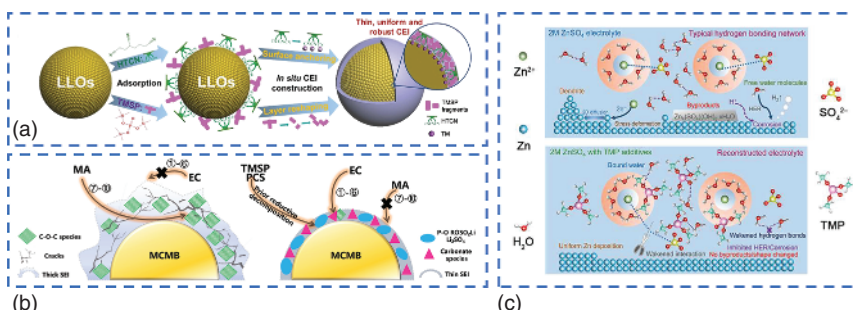


Figure 1.8 Functions of phosphate ester in electrolytes. (a) Schematic illustration of the synergistic effects of HTCN + TMSP on adjusting the CEI structure and cathode electrochemistry. Source: Reproduced from Zhao et al. [130]/with permission of Wiley-VCH Verlag GmbH & Co. KGaA. (b) The possible working mechanism of TMSP and PCS functional additives. Source: Reproduced from Xu et al. [131]/with permission of Elsevier. (c) Schematic illustration of TMP additives to optimize electrolyte/anode interface. Source: Reproduced from Zhang et al. [132]/with permission of Elsevier.

of the NCM111 cathode changed significantly in the electrolyte without TMSP but maintained its morphology with TMSP. XPS results indicated that even with TMSP, the main component of CEI was still the decomposition product of the electrolyte rather than TMSP, indicating that TMSP was not directly involved in the formation of CEI to protect the cathode. Instead, it was regarded as a method of protecting the cathode material through the occurrence of the P—O—M (M = Ni, Co and Mn) complexation on the cathode surface, which resulted in a milder environment at the electrode interface. Therefore, the stabilizing mechanism of TMSP on the cathode still needs to be further explored.

TMSP can also participate in the formation of SEI of graphite anode due to the reactivity of TMSP with lithium alkyl oxides formed during EC degradation [134]. Xu et al. [131] introduced TMSP and 1,3-propanediolcyclic sulfate (PCS) into a carbonate electrolyte with methyl acetate (MA) as a cosolvent. It was found that the surface of the graphitic mesocarbon microbeads (MCMB) anode was smooth after cycling with TMSP and PCS, indicating the formation of a thin and dense SEI layer. The results of XPS on the cycled MCMB electrode revealed that TMSP and PCS would be reduced on the MCMB anode to generate P—O, ROSO_2Li , and Li_2SO_4 , covering the $\text{CH}_3\text{O}\bullet$ and C—O—C generated from the decomposition of MA to form a stable SEI (Figure 1.8b).

In addition, some fluorinated phosphate esters are endowed with the ability to participate in the formation of SEI and CEI due to the strong electronegativity of their F atoms. Sun et al. [127] introduced THFP as an additive into a flame-retardant electrolyte and found that THFP would decompose on the surface of NCM622 cathode to form the thin and dense CEI rich in C—F, and the lithium-philic properties of C—F bond would guide the uniform distribution of lithium-ion flux in the CEI layer to improve the cycling stability. Moreover, the strong electron-withdrawing F atoms can reduce the LUMO of phosphate esters, which leads to the preferential reduction of THFP on the lithium surface to form a LiF-rich SEI. In addition to the outstanding film-forming properties, THFP can also dissociate LiPF_6 salts through strong bonding with the PF_6^- , facilitating the migration of lithium ions in the electrolyte and modulating the structure and composition of the SEI. Therefore, fluorinated phosphate esters are often introduced into electrolytes as multifunctional additives to improve the thermal and cycling stability of batteries.

1.5.1.3 Involvement in Solvation Structure Regulation

Phosphate ester additives can also regulate the solvation structure of cations in LIBs, potassium ion batteries, and even aqueous zinc-ion batteries. Gao et al. [135] introduced TFP into potassium-ion batteries and found that TFP with weak solvation ability and high oxidative stability could weaken the interaction of solvent molecules with K^+ , thereby promoting the retention of FSI^- anions in the solvation sheath of K^+ to form an anion-rich solvation structure to generate anion-derived SEI. In addition, the corrosion of potassium bis(fluoromethanesulfonyl)imide (KFSI)-based electrolytes to the Al collector was suppressed due to the weak solubility of TFP.

In aqueous batteries, phosphate esters are also often used as green and environmentally friendly additives to modulate the solvation structure. Zhang et al. [132] systematically investigated the interaction between phosphate esters and aqueous electrolytes and found that TMP with the highest dielectric constant and the smallest molecular volume among a series of phosphate esters could be easily intercalated into the solvation structure of Zn^{2+} (Figure 1.8c). In addition, abundant theoretical calculations and experimental characterizations proved that TMP molecules could not only modify the solvated structure but also get preferentially adsorbed on the Zn electrode surface to optimize EDL. As a result, a zincophilic–hydrophobic inorganic–organic interface layer was formed, enabling multiple locking of water molecules while thermodynamically and kinetically guarding a continuous and stable zinc plating/stripping process.

1.5.2 Drawbacks of Phosphate Ester

1.5.2.1 Incompatibility with Anodes

Although phosphate ester additives have flame-retardant properties, researchers have revealed phosphate ester additives with low concentrations in the electrolyte are insufficient to act as a flame retardant, and phosphate ester additives with high concentrations tend to decompose on graphite, lithium metal, or sodium metal anodes. The decomposition of phosphate ester participated in the formation of an unstable SEI with poor electronic shielding ability, which had troubles in effectively preventing the coinserting of Li^{+} -solvent and the continuous decomposition of solvent, further leading to the reduction of battery capacity and poor cycle stability [136]. For graphite anodes, the decomposition of phosphate ester on the anode will lead to delamination and flaking of the graphite electrode, and due to the strong catalytic effect on the surface of the graphite anode, it will further lead to the continuous decomposition of the phosphate ester solvent, which is detrimental to the cycle stability of the battery [137].

1.5.2.2 Improvement of the Compatibility of Phosphate Ester and Lithium Metal

1) Introduction of SEI-forming agent

$LiDFOB$, $LiPF_6$, and other lithium salts are commonly used in electrolytes with excellent SEI-forming properties. Li et al. [126] found through characterization by XPS and high-resolution cryo-electron microscopy (cryo-EM) that the thickness of the SEI layer derived from lithium salt without $LiDFOB$ reached 45 nm in thickness. The mosaic SEI layer was randomly distributed with Li_2O , Li_3PO_4 , and Li_2CO_3 crystal particles. In contrast, the amorphous layer was mainly composed of low molecular weight organic substances, such as P—O and C—O. The uneven SEI would further lead to uneven Li deposition and result in the growth of lithium dendrites. In contrast, the SEI layer derived with $LiDFOB$ lithium salts was only 13.6 nm, forming a uniform Li_2O /polymer SEI layer, and this uniform SEI prevented the electron tunneling of the Li anode and inhibited the further reaction of the highly active TEP molecules with the lithium metal.

As mentioned earlier, FEC is one of the most widely used SEI-forming agents. Ma et al. [138] introduced FEC into the TEP-based electrolyte of Na metal batteries. FEC could promote the formation of a robust SEI layer on the anode surface, relieving the interfacial reactivity between the phosphate ester-based electrolytes and the Na metal anode. Through the optimization of the ratio of TEP to FEC, phosphate ester-based electrolytes with high oxidative stability and nonflammability could realize the stable cycle of Na metal batteries. In lithium-sulfur batteries, FEC can still protect the stability of the phosphate ester-based electrolyte through preferential decomposition at the anode. Wang et al. [139] introduced FEC and $\text{Sn}(\text{OTf})_2$ additives into a TEP-based electrolyte, and $\text{Sn}(\text{OTf})_2$ optimized the solvation structure of Na^+ and promoted the TFSI^- to replace a portion of the TEP to participate in the solvation structure (Figure 1.9a), effectively reducing the desolvation energy barrier of Na^+ . In addition, FEC could preferentially decompose on the anode to form a stable SEI film, thus inhibiting the decomposition of TEP. The synergistic effect of FEC and $\text{Sn}(\text{OTf})_2$ effectively enhanced the stability of TEP-based electrolytes and their compatibility with Na metal.

2) Regulation of solvation structures

Modification of the solvation structure can be achieved by regulating the composition of the electrolyte, thus improving the compatibility of the electrolyte with the anode. Liu et al. [136] explored the ratio of lithium salt, TEP, and EC and found that EC could stabilize TEP in the electrolyte and ensure the compatibility of the electrolyte with the graphite anode when the molar ratio of lithium salt to TEP was 1 : 2. However when the molar ratio of the lithium salt to TEP changed to 1 : 3, it was difficult to regulate the solvation structure of TEP by introducing EC, as shown in Figure 1.9b. Therefore, through the competitive coordination between TEP and EC, a dynamically stable solvation structure could be constructed to weaken the decomposition of TEP and realize a balance between electrolyte flame retardancy and electrochemical stability.

Zeng et al. [121] also found by regulating the molar ratio of salt to solvent that Li^+ was more inclined to be complexed with $\text{P}=\text{O}$ in four TEP molecules to form tetrahedral complexes when the molar ratio of lithium bis(fluorosulfonyl)imide (LiFSI) and TFP was $<1 : 4$, and Li^+ preferred to form an “ion-solvent” complex structure with two TEP molecules and two $\text{S}=\text{O}$ groups of FSI^- when the molar ratio was $>1 : 2$. The results showed that when the molar ratio of LiFSI and TFP was high, there were fewer free solvent molecules in the electrolyte, resulting in a negative shift of the solvent reduction potential and inhibiting the decomposition of solvent molecules on the anode surface. However, LiFSI with excessive concentration would cause the increased viscosity of electrolytes and decreased electrochemical performance. Therefore, when the molar ratio of LiFSI to TEP was 1 : 2, the system had lower viscosity and higher ionic conductivity, which could inhibit the irreversible decomposition of solvent and realize the reversible electrochemical cycle of lithium metal anode.

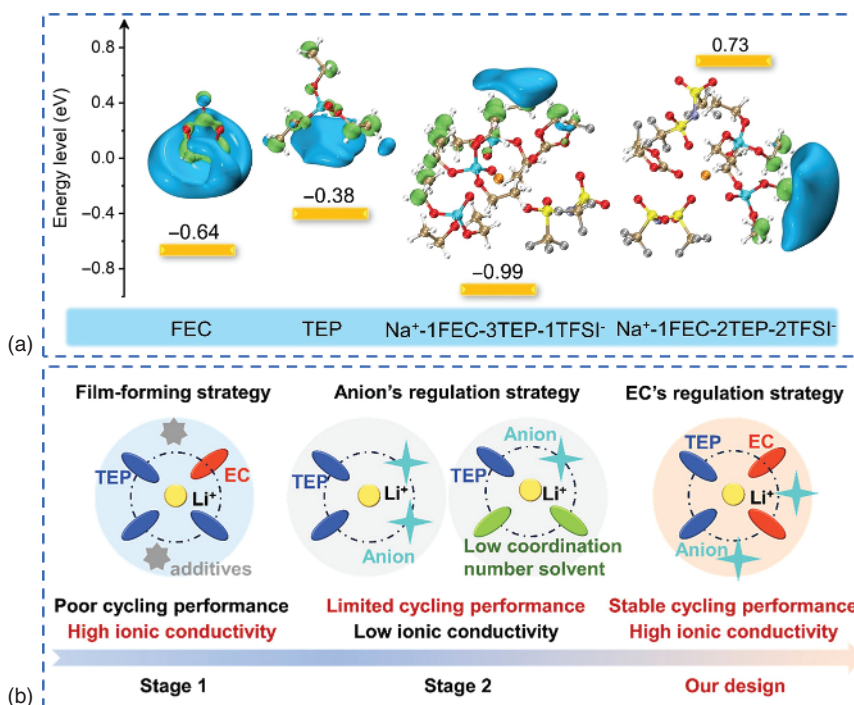


Figure 1.9 Solutions to optimize the compatibility of phosphate ester with anode. (a) LUMO energy level of FEC, TEP, Na^+ -1FEC-3STEP-1TFSI⁻ and Na^+ -1FEC-2TEP-2TFSI⁻. Source: Reproduced from Wang et al. [139]/with permission of Wiley-VCH Verlag GmbH & Co. KGaA. (b) Features of reported TEP-modified nonflammable electrolytes, their solvation structure models, and the performance of Gr electrodes. Source: Reproduced from Liu et al. [136]/with permission of American Chemical Society.

1.6 Sulfate Ester Additives

1.6.1 Functions of Sulfate Ester Additives

1.6.1.1 SEI-Forming Additives

Sulfate ester is a novel SEI-forming additive with a low LUMO energy level, which can be preferentially reduced and decomposed on the anode surface to form SEI film during cycling. 1,3-Propane sultone (1,3-PS), 1,4-butane sultone (1,4-BS), ethylene sulfate (DTD), and ethylene sulfite (ES) have been investigated for applications in the formation of SEI.

Xu et al. [140] investigated the film-forming performance of 1,4-BS as a novel sulfate ester additive in nonaqueous electrolytes for the first time in 2007. It was found by CV scanning that the electrolyte introduced with 1,4-BS showed a reduction peak at 0.7 V, which might be due to the reduction of 1,4-BS to form SEI film on the surface of the graphite anode. The peak disappeared in the second sweeping, indicating that the 1,4-BS-derived SEI film had been stably formed in the first sweeping and could effectively inhibit the further reduction of the electrolyte on the graphite electrode.

A small amount of 1,4-BS could form a dense and stable SEI film on the surface of the graphite anode, which effectively prevented propylene carbonate and solvation lithium ions from coinsertion into graphite, thereby overcoming the drawbacks of propylene carbonate such as capacity loss and decline in cycle stability. The introduction of 1,4-BS as an additive could change the composition of the SEI film and improve the stability of SEI film and the electrochemical performance of LIBs. Since the structure of 1,3-PS is similar to that of 1,4-BS, Xu et al. also investigated the functions of 1,3-PS in the electrolyte using a similar method in 2009 and found the S element in SEI using XPS characterization, confirming that 1,3-PS indeed involved in the formation of SEI film [141].

Sano et al. [142] systematically investigated the functions of DTD and its derivatives in electrolytes. First, through the CV test, it was found that the reduction current of the electrolyte with DTD was lower than that without DTD, indicating that the DTD decomposition products formed SEI on the surface of the graphite anode, which prevents the decomposition of PC. In addition, the anodic peak with DTD was higher than that without DTD, probably because the decomposition products of DTD prevented the graphite stripping that accompanied the decomposition of PC, which increased the reversible capacity and the anodic current. The charge-discharge curves of the DTD derivatives showed that the initial efficiency of methyl DTD (MDTD) was the same as that of DTD, but the initial efficiency of ethyl DTD (EDTD) was low, indicating that the longer alkyl chain might reduce the performance of SEI. In addition, researchers found that DTD possessed better performance than ES, which had a similar structure to DTD. Therefore, DTD and its alkyl derivatives may be able to replace ES as more efficient SEI-forming additives to effectively inhibit the initial capacity loss of batteries, reduce the expansion of batteries after high-temperature standing, and improve the charging and discharging performance of batteries. Hall et al. [143] found that the reduction onset potential of DTD was related to its addition amount, and the reduction potential of DTD was lower than that of EC based on the differential capacity (dQ/dV) test. It was confirmed that DTD would be preferentially reduced at the anode and participate in the formation of SEI. Li et al. [144] further demonstrated the degradation products of DTD using XPS and found that the SEI formed by the electrolyte with DTD was rich in LiSO_3 and ROSO_2Li . The inorganic-rich SEI was the key to the reduction of the interface impedance of the battery with DTD.

Previously, researchers proposed the preferential decomposition of DTDs to participate in the formation of SEIs but did not mention the prerequisites required to exert the role of DTDs. Cheng et al. [145] proposed the unique function of DTDs and revealed the prerequisite of solvation for effectively weakening Li^+ -solvent interaction in electrolytes for the first time. It was shown that when DTDs with high polar surface area (PSA) and strong coordination of Li^+ were introduced into the flame-retardant TMP-based electrolytes, the DTDs would not weaken the Li^+ -TMP interaction. TMP with a low dielectric constant ($\epsilon = 21.3$) possessed weak dissociation ability for LiPF_6 , unable to dissociate Li^+ and PF_6^- ions in the electrolyte completely. Therefore, DTDs were challenging to coordinate with Li^+ .

and existed near the second solvation sheath, failing to inhibit Li^+ -TMP interactions. In contrast, when EC with high dielectric constant and strong solvation ability was introduced into the electrolyte, DTD was able to enter the first solvation sheath and coordinate with Li^+ to inhibit Li^+ -TMP interactions due to the strong dissociation of LiPF_6 by EC (Figure 1.10a). With the gradual addition of DTD, EMC, and EC, the content of TMP molecules in the solvation structure of lithium ions gradually decreased while the content of DTD increased, indicating the strengthened Li^+ -DTD interactions and weakened Li^+ -TMP interactions were achieved through the regulation of solvents and additives. Therefore, when using DTD as an electrolyte additive, we need to pay attention to the dielectric constant of the solvent in the electrolyte, ensuring the prerequisite conditions for the dissociation of lithium salts to enable DTD to perform its function.

ES is structurally similar to VC and has been used in LMBs to form stable SEI. It can effectively inhibit the coinsertion behavior of propylene carbonate when used as a solvent or co-solvent [148]. Pham et al. [149] used ES and DES as electrolytes, and ES possesses a high boiling point (173°C), low melting point (-11°C), and high dielectric constant (41.0). However, ES with a high dielectric constant has strong solvation ability, thus forming a solvation structure dominated by solvent, which is not conducive to forming rich inorganic SEI. Therefore, DES with a low dielectric constant (16.2) was introduced to balance the solvation ability of the mixed solvents. In the electrolyte with sulfate ester, an anion-rich solvation structure was formed due to the low dielectric constant of DES, resulting in an anion-derived SEI rich in inorganic components LiF as well as LiPS , which were mainly produced by the decomposition of phosphate esters. These inorganic components played a crucial role in passivating lithium deposition, inhibiting dendrite formation, and ultimately improving the electrochemical performance of batteries. In contrast, the SEI formed by the carbonate electrolyte was mainly composed of organic components with poor ionic conductivity and mechanical strength. It could be concluded that the phosphate ester-based electrolytes are able to produce stable and robust SEIs and improve the coulomb efficiency and cycle stability of batteries. Liu et al. [146] revealed that electrolytes with dimethyl sulfite (DMS) and diethyl sulfite (DES) exhibited excellent compatibility with composite SiO/C anodes. The sulfide-rich SEI with low impedance was formed on the surface of the anode through pre-cycling, which could inhibit the oxidative decomposition of sulfur-containing organic solvents at higher potentials during the subsequent cycling process (Figure 1.10b). In addition, this sulfide-rich, SEI-modified layer endowed the battery with cycling stability performance at low temperatures, which was of great significance in promoting the development of low-temperature lithium batteries.

1.6.1.2 CEI-Forming Additives

Sulfur-containing compounds can also be used as CEI-forming agents due to their natural insolubility and the high oxidative stability of sulfates, like Li_2SO_4 and ROSO_3Li . Kim et al. [150] showed through theoretical calculation that the $-\text{S}(\text{=O})_2-$, $-\text{OS}(\text{=O})_2-$ and $-\text{OS}(\text{=O})_2\text{O}-$ groups in sulfur-containing compounds and their decomposition products could be complexed with the

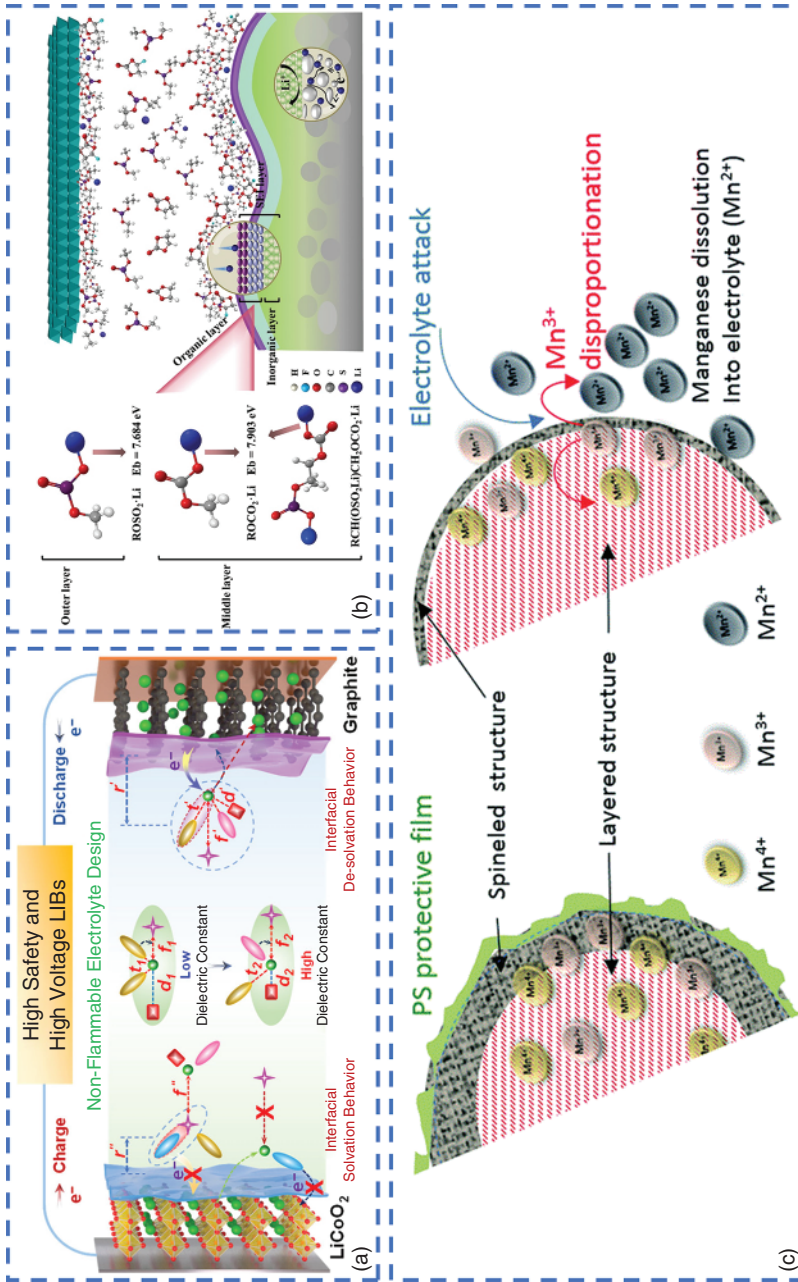


Figure 1.10 SEI and CEI forming properties of sulfate. (a) Schematics illustrating solvation structure and interfacial model in designed electrolytes. Source: Reproduced from Cheng et al. [145] with permission of American Chemical Society. (b) The binding energy for Li^+ with organic components in a modified layer by DFT and simulation model of MD in the battery. Source: Liu et al. [146]/John Wiley & Sons/CC BY 4.0. (c) A schematic of the PS protection mechanism on the Li-rich NMC cathode during cycling and progressive transformation from the layered to the spinel structure. Source: Reproduced from Pires et al. [147]/with permission of Royal Society of Chemistry.

transition metal (Ni^{2+}) in the cathode, thus enhancing the structural stability of the Ni-containing cathodes, improving the interfacial stability of the cathode and electrolytes, and inhibiting the dissolution of the transition metal atoms.

DTD has been proven to be applied to lithium metal and graphite anodes to form stabilized SEIs, while it can also be decomposed on the cathode to generate CEIs. Ren et al. [151] added DTD to Na—S batteries, where a ring-opened intermediate was created between the electrophilic DTD additive and Na_2S_x ($1 \leq x \leq 8$). The intermediate was an organic sodium salt, consisting of a PS and a sulfate group, which were linked by a $-\text{CH}_2-\text{CH}_2-$ group. When the sodium salt intermediate aggregated in a solvent with low DN, such as DME, PS and sulfate reacted to form insoluble polymeric products, explaining the formation of an interphase layer. Instead, in the solvent with high DN, the anion would be separated by a solvent and would not be in direct contact with other anions. Therefore, there was no aggregation-induced polymerization, explaining why the organic sodium salt could be dissolved in the solvent with high DN. As a result, the DTD additives spontaneously reacted with sodium sulfide to form a robust sulfate-based CEI on the sulfated polyacrylonitrile cathode, which protected the cathode and inhibited the dissolution of sodium polysulfide.

Due to the high oxidation state of the sulfur atom in 1,3-PS, its decomposition products can be more stable at high potentials and match with high-voltage cathodes [152]. Pires et al. [147] added 1,3-PS to the electrolyte of high-voltage LIB and found that 1,3-PS could form a protective film with a wide electrochemical stable window (5.0 V) on the surface of Li-rich-NMC cathode, which effectively suppressed the occurrence of side reactions on the electrode surface as well as the dissolution of the metal ions (Figure 1.10c). Similar to 1,3-PS, prop-1-ene-1,3-sultone (PES) can also be used as a CEI-forming agent in high-voltage LIBs. Li et al. [153] introduced PSE into the electrolyte and demonstrated that PSE formed a protective CEI film on the LNMO cathode, which inhibited the decomposition of the electrolyte on the cathode surface, improved the interfacial properties between the cathode and electrolyte, and significantly enhanced the cycling stability of LNMO. With the addition of 1 wt% PES, the capacity retention rate increased from 49% to 90% after 400 cycles at the rate of 1C.

Methylene methanedisulfonate (MMDS) is also capable of improving the cycling stability of batteries at high voltage, which not only forms a stable SEI film on the graphite anode but also facilitates the formation of a thin CEI to improve the performance of batteries. Zuo et al. [154] showed that the electrolyte without MMDS was decomposed at 5.3 V, while the electrolyte with 0.5 wt% MMDS was oxidized at 5.1 V through LSV tests. A decrease in the oxidation potential indicated that MMDS might decompose on the LCO cathode before the solvent, so as to inhibit the decomposition of the electrolyte. A further CV test showed that two reduction peaks appeared at 3.6 and 3.8 V in the electrolyte with MMDS, which were attributed to the insertion of lithium ions into LCO and the decomposition of MMDS on the LCO cathode to form a CEI, respectively. It was observed by TEM that the thickness of CEI obtained with MMDS was only 3–5 nm, compared with that formed without MMDS (15–20 nm), and the thinner CEI could reduce the surface impedance and thus improve the cycling performance of the battery.

1.7 Conclusion and Outlook

After the discussion of the functions of widely used electrolyte additives, we can find that electrolyte additives, as a core component of electrolytes, directly affect the overall performance and safety of batteries. With the rapid expansion of markets for electric vehicles, smartphones, and other electronic products, there is a growing demand for batteries with high energy density, long cycle life, and stable safety performances, so it is essential to carry out continuous research and optimization of the functions and performances of electrolytes additives.

Currently, the functions of electrolyte additives are mainly concentrated in the following aspects:

i) SEI and CEI film-forming agents.

Additives with low LUMO and high HOMO can be preferentially decomposed on the electrode surface, which prevents the excessive decomposition of the electrolyte on the electrodes. Some additives can regulate the solvation sheath to form anion-rich solvation structures, which also essentially facilitates the formation of inorganic-rich SEIs.

ii) Improvement of ion transport.

Nitrile compounds can act as plasticizers in polymer-based electrolytes and ionic transport carriers in nitrile compounds-rich electrolytes, thereby facilitating the transport of ions.

iii) Flame retardant.

For flammable and explosive electrolytes, the addition of flame retardants, like phosphate esters, is crucial to improve the thermal stability of batteries effectively.

However, although the application of additives has achieved certain results, the employment of electrolyte additives is still limited, and the stability of electrolytes in extreme environments, like high temperature and high pressure, needs to be improved. Moreover, the action mechanism of some additives is still unclear and still needs further exploration and research.

Therefore, we consider that future research on electrolyte additives should be mainly focused on the following aspects:

- i) the development of novel additives to meet the requirements of extreme conditions of battery systems;
- ii) in-depth research on the action mechanism of additives to provide theoretical support for the optimization of the design of additives;
- iii) to strengthen the study on synergistic effects of additives with electrolytes, electrodes, and other components of batteries to achieve the optimization of the overall performance of batteries.

In summary, research on electrolyte additives is of great significance for improving the performance and safety of batteries. Although the current research has achieved certain results, there are still many challenges and problems to be solved to promote the application of battery electrolyte additives in industrial production.

References

- 1 Zhang, S., Li, S., Wang, X. et al. (2023). Nonflammable electrolyte with low exothermic design for safer lithium-based batteries. *Nano Energy* 114: 108639.
- 2 Meng, Y., Zhou, D., Liu, R. et al. (2023). Designing phosphazene-derivative electrolyte matrices to enable high-voltage lithium metal batteries for extreme working conditions. *Nature Energy* 8: 1023–1033.
- 3 Kim, M.-H., Wi, T.-U., Seo, J. et al. (2023). Design principles for fluorinated interphase evolution via conversion-type alloying processes for anticorrosive lithium metal anodes. *Nano Letters* 23: 3582–3591.
- 4 Yu, Y., Wang, S., Zhang, J. et al. (2023). Long-life lithium batteries enabled by a pseudo-oversaturated electrolyte. *Carbon Energy* 6: e383.
- 5 Li, G.-X., Jiang, H., Kou, R. et al. (2022). A superior carbonate electrolyte for stable cycling Li metal batteries using high Ni cathode. *ACS Energy Letters* 7: 2282–2288.
- 6 Aurbach, D., Markevich, E., and Salitra, G. (2021). High energy density rechargeable batteries based on Li metal anodes. The role of unique surface chemistry developed in solutions containing fluorinated organic co-solvents. *Journal of the American Chemical Society* 143: 21161–21176.
- 7 Cui, Z., Zou, F., Celio, H. et al. (2022). Paving pathways toward long-life graphite/LiNi0.5Mn1.5O4 full cells: electrochemical and Interphasial points of view. *Advanced Functional Materials* 32: 2203779.
- 8 Li, Z., Tang, W., Deng, Y. et al. (2022). Enabling highly stable lithium metal batteries by using dual-function additive catalyzed in-built quasi-solid-state polymer electrolytes. *Journal of Materials Chemistry A* 10: 23047–23057.
- 9 Lin, R., He, Y., Wang, C. et al. (2022). Characterization of the structure and chemistry of the solid–electrolyte interface by cryo-EM leads to high-performance solid-state Li-metal batteries. *Nature Nanotechnology* 17: 768–776.
- 10 Liao, C., Han, L., Wang, W. et al. (2023). Non-flammable electrolyte with lithium nitrate as the only lithium salt for boosting ultra-stable cycling and fire-safety lithium metal batteries. *Advanced Functional Materials* 33: 2212605.
- 11 Shin, H., Park, J., Sastry, A.M. et al. (2015). Effects of fluoroethylene carbonate (FEC) on anode and cathode interfaces at elevated temperatures. *Journal of the Electrochemical Society* 162: A1683–A1692.
- 12 Li, Z., Yao, N., Yu, L. et al. (2023). Inhibiting gas generation to achieve ultralong-lifespan lithium-ion batteries at low temperatures. *Matter* 6: 2274–2292.
- 13 Guo, X.F., Yang, Z., Zhu, Y.F. et al. (2022). High-voltage, highly reversible sodium batteries enabled by fluorine-rich electrode/electrolyte interphases. *Small Methods* 6: 2200209.
- 14 Su, C.-C., He, M., Amine, R. et al. (2019). Cyclic carbonate for highly stable cycling of high voltage lithium metal batteries. *Energy Storage Materials* 17: 284–292.

15 Fu, C., Ma, Y., Lou, S. et al. (2020). A dual-salt coupled fluoroethylene carbonate succinonitrile-based electrolyte enables Li-metal batteries. *Journal of Materials Chemistry A* 8: 2066–2073.

16 Li, Y., Li, Y., Pei, A. et al. (2017). Atomic structure of sensitive battery materials and interfaces revealed by cryo-electron microscopy. *Science* 358: 506–510.

17 Yan, C., Cheng, X.B., Tian, Y. et al. (2018). Dual-layered film protected lithium metal anode to enable dendrite-free lithium deposition. *Advanced Materials* 30: 1707629.

18 Liu, J., Yuan, B., He, N. et al. (2023). Reconstruction of LiF-rich interphases through an anti-freezing electrolyte for ultralow-temperature LiCoO_2 batteries. *Energy & Environmental Science* 16: 1024–1034.

19 Tao, M., Xiang, Y., Zhao, D. et al. (2022). Quantifying the evolution of inactive Li/lithium hydride and their correlations in rechargeable anode-free Li batteries. *Nano Letters* 22: 6775–6781.

20 Zhang, W., Yang, T., Liao, X. et al. (2023). All-fluorinated electrolyte directly tuned Li^+ solvation sheath enabling high-quality passivated interfaces for robust Li metal battery under high voltage operation. *Energy Storage Materials* 57: 249–259.

21 Wang, Y., Zhang, Y., Dong, S. et al. (2022). An all-fluorinated electrolyte toward high voltage and long cycle performance dual-ion batteries. *Advanced Energy Materials* 12: 2103360.

22 Lu, H., He, L., Yuan, Y. et al. (2020). Synergistic effect of fluorinated solvents for improving high voltage performance of $\text{LiNi}_{0.5}\text{Mn}_{1.5}\text{O}_4$ cathode. *Journal of the Electrochemical Society* 167: 120534.

23 Nagarajan, S., Weiland, C., Hwang, S. et al. (2022). Depth-dependent understanding of cathode electrolyte interphase (CEI) on the layered Li-ion cathodes operated at extreme high temperature. *Chemistry of Materials* 34: 4587–4601.

24 Hernández, G., Mogensen, R., Younesi, R. et al. (2022). Fluorine-free electrolytes for lithium and sodium batteries. *Batteries & Supercaps* 5: e202100373.

25 Su, C.-C., He, M., Amine, R. et al. (2019). Solvating power series of electrolyte solvents for lithium batteries. *Energy & Environmental Science* 12: 1249–1254.

26 Chen, L., Nian, Q., Ruan, D. et al. (2023). High-safety and high-efficiency electrolyte design for 4.6 V-class lithium-ion batteries with a non-solvating flame-retardant. *Chemical Science* 14: 1184–1193.

27 Su, C.C., He, M., Shi, J. et al. (2020). Solvation rule for solid-electrolyte interphase enabler in lithium-metal batteries. *Angewandte Chemie International Edition* 59: 18229–18233.

28 Weng, S., Yang, G., Zhang, S. et al. (2023). Kinetic limits of graphite anode for fast-charging lithium-ion batteries. *Nano-Micro Letters* 15: 215.

29 Su, C.-C., He, M., Cai, M. et al. (2022). Solvation-protection-enabled high-voltage electrolyte for lithium metal batteries. *Nano Energy* 92: 106720.

30 Wang, C., Sun, Z., Liu, L. et al. (2023). A rooted interphase on sodium via in situ pre-implantation of fluorine atoms for high-performance sodium metal batteries. *Energy & Environmental Science* 16: 3098–3109.

31 Yang, X., Cheng, F., Yang, Z. et al. (2023). Multifunctionalizing electrolytes in situ for lithium metal batteries. *Nano Energy* 116: 108825.

32 Zhang, W., Koverga, V., Liu, S. et al. (2024). Single-phase local-high-concentration solid polymer electrolytes for lithium-metal batteries. *Nature Energy* 9: 386–400.

33 Biswal, P., Rodrigues, J., Kludze, A. et al. (2022). A reaction-dissolution strategy for designing solid electrolyte interphases with stable energetics for lithium metal anodes. *Cell Reports Physical Science* 3: 100948.

34 Huang, W., Wang, Y., Lv, L. et al. (2021). 1-Hydroxyethylidene-1,1-diphosphonic acid: a multifunctional interface modifier for eliminating HF in silicon anode. *Energy Storage Materials* 42: 493–501.

35 Yang, X., Lin, M., Zheng, G. et al. (2020). Enabling stable high-voltage LiCoO₂ operation by using synergistic interfacial modification strategy. *Advanced Functional Materials* 30: 2004664.

36 Shen, C., Wang, S., Jin, Y. et al. (2015). In situ AFM imaging of solid electrolyte interfaces on HOPG with ethylene carbonate and fluoroethylene carbonate-based electrolytes. *ACS Applied Materials & Interfaces* 7: 25441–25447.

37 Xia, L., Lee, S., Jiang, Y. et al. (2017). Fluorinated electrolytes for Li-ion batteries: the lithium difluoro(oxalato)borate additive for stabilizing the solid electrolyte interphase. *ACS Omega* 2: 8741–8750.

38 Aktekin, B., Younesi, R., Zipprich, W. et al. (2017). The effect of the fluoroethylene carbonate additive in LiNi_{0.5}Mn_{1.5}O₄-Li₄Ti₅O₁₂ lithium-ion cells. *Journal of the Electrochemical Society* 164: A942–A948.

39 Tan, J., Ye, M., and Shen, J. (2022). Deciphering the role of LiNO₃ additives in Li-S batteries. *Materials Horizons* 9: 2325–2334.

40 Zhou, P., Hou, W., Xia, Y. et al. (2023). Tuning and balancing the donor number of lithium salts and solvents for high-performance Li metal anode. *ACS Nano* 17: 17169–17179.

41 Fang, W., Wen, Z., Chen, L. et al. (2022). Constructing inorganic-rich solid electrolyte interphase via abundant anionic solvation sheath in commercial carbonate electrolytes. *Nano Energy* 104: 107881.

42 Cai, T., Sun, Q., Cao, Z. et al. (2022). Electrolyte additive-controlled interfacial models enabling stable antimony anodes for lithium-ion batteries. *The Journal of Physical Chemistry C* 126: 20302–20313.

43 Huang, G., Liao, Y., Zhao, X. et al. (2022). Tuning a solvation structure of lithium ions coordinated with nitrate anions through ionic liquid-based solvent for highly stable lithium metal batteries. *Advanced Functional Materials* 33: 2211364.

44 Zhu, Y., Li, X., Si, Y. et al. (2022). Regulating dissolution chemistry of nitrates in carbonate electrolyte for high-stable lithium metal batteries. *Journal of Energy Chemistry* 73: 422–428.

45 Wahyudi, W., Ladelta, V., Tsetseris, L. et al. (2021). Lithium-ion desolvation induced by nitrate additives reveals new insights into high performance lithium batteries. *Advanced Functional Materials* 31: 2101593.

46 Fu, J., Ji, X., Chen, J. et al. (2020). Lithium nitrate regulated sulfone electrolytes for lithium metal batteries. *Angewandte Chemie International Edition* 59: 22194–22201.

47 Fan, X., Chen, L., Ji, X. et al. (2018). Highly fluorinated interphases enable high-voltage Li-metal batteries. *Chem* 4: 174–185.

48 Yamada, Y., Wang, J., Ko, S. et al. (2019). Advances and issues in developing salt-concentrated battery electrolytes. *Nature Energy* 4: 269–280.

49 Ren, X., Zou, L., Cao, X. et al. (2019). Enabling high-voltage lithium-metal batteries under practical conditions. *Joule* 3: 1662–1676.

50 Stuckenbergs, S., Bela, M.M., Lechtenfeld, C.T. et al. (2023). Influence of LiNO₃ on the lithium metal deposition behavior in carbonate-based liquid electrolytes and on the electrochemical performance in zero-excess lithium metal batteries. *Small* 20: 2305203.

51 Zheng, T., Zhu, B., Xiong, J. et al. (2023). When audience takes stage: pseudo-localized-high-concentration electrolyte with lithium nitrate as the only salt enables lithium metal batteries with excellent temperature and cathode adaptability. *Energy Storage Materials* 59: 102782.

52 Ma, X., Yu, J., Zou, X. et al. (2023). Single additive to regulate lithium-ion solvation structure in carbonate electrolytes for high-performance lithium-metal batteries. *Cell Reports Physical Science* 4: 101379.

53 Fu, L., Wang, X., Wang, L. et al. (2021). A salt-in-metal anode: stabilizing the solid electrolyte interphase to enable prolonged battery cycling. *Advanced Functional Materials* 31: 2010602.

54 Hou, L.P., Yao, N., Xie, J. et al. (2022). Modification of nitrate ion enables stable solid electrolyte interphase in lithium metal batteries. *Angewandte Chemie International Edition* 61: e202201406.

55 Zhang, Q., Xu, L., Yue, X. et al. (2023). Catalytic current collector design to accelerate LiNO₃ decomposition for high-performing lithium metal batteries. *Advanced Energy Materials* 13: 2302620.

56 Zhang, Z., Wang, J., Zhang, S. et al. (2021). Stable all-solid-state lithium metal batteries with Li₃N-LiF-enriched interface induced by lithium nitrate addition. *Energy Storage Materials* 43: 229–237.

57 Kim, S., Lee, T.K., Kwak, S.K. et al. (2021). Solid electrolyte interphase layers by using lithiophilic and electrochemically active ionic additives for lithium metal anodes. *ACS Energy Letters* 7: 67–69.

58 Cheng, X.B., Yang, S.J., Liu, Z. et al. (2023). Electrochemically and thermally stable inorganics-rich solid electrolyte interphase for robust lithium metal batteries. *Advanced Materials* 36: 2307370.

59 Jung, T.-J., Lee, H., Park, S.H. et al. (2022). Statistical and computational analysis for state-of-health and heat generation behavior of long-term cycled LiNi_{0.8}Co_{0.15}Al_{0.05}O₂/graphite cylindrical lithium-ion cells for energy storage applications. *Journal of Power Sources* 529: 231240.

60 Wang, K., Ni, W., Wang, L. et al. (2023). Lithium nitrate regulated carbonate electrolytes for practical Li-metal batteries: mechanisms, principles and strategies. *Journal of Energy Chemistry* 77: 581–600.

61 Liu, S., Xia, J., Zhang, W. et al. (2022). Salt-in-salt reinforced carbonate electrolyte for Li metal batteries. *Angewandte Chemie International Edition* 61: e202210522.

62 Liang, Y., Wu, W., Li, D. et al. (2022). Highly stable lithium metal batteries by regulating the lithium nitrate chemistry with a modified eutectic electrolyte. *Advanced Energy Materials* 12: 2202493.

63 Jiang, Z., Yang, T., Li, C. et al. (2023). Synergistic additives enabling stable cycling of ether electrolyte in 4.4 V Ni-rich/Li metal batteries. *Advanced Functional Materials* 33: 2306868.

64 Wen, Z., Fang, W., Wang, F. et al. (2024). Dual-salt electrolyte additive enables high moisture tolerance and favorable electric double layer for lithium metal battery. *Angewandte Chemie International Edition* 63: e202314876.

65 Li, X., Zhao, R., Fu, Y. et al. (2021). Nitrate additives for lithium batteries: mechanisms, applications, and prospects. *eScience* 1: 108–123.

66 Coke, K., Johnson, M.J., Robinson, J.B. et al. (2024). Illuminating polysulfide distribution in lithium sulfur batteries; tracking polysulfide shuttle using operando optical fluorescence microscopy. *ACS Applied Materials & Interfaces* 16: 20329–20340.

67 Kim, S., Jung, J., Kim, I. et al. (2023). Tuning of electrolyte solvation structure for low-temperature operation of lithium–sulfur batteries. *Energy Storage Materials* 59: 102763.

68 Zhang, X., Wang, Y., Ouyang, Z. et al. (2023). Dual-functional lithium nitrate mediator eliminating water hazard for practical lithium metal batteries. *Advanced Energy Materials* 14: 2303048.

69 Wang, Z., Hou, L.P., Li, Z. et al. (2022). Highly soluble organic nitrate additives for practical lithium metal batteries. *Carbon Energy* 5: e283.

70 Wang, Z., Wang, Y., Shen, L. et al. (2023). Towards durable practical lithium–metal batteries: advancing the feasibility of poly-DOL-based quasi-solid-state electrolytes via a novel nitrate-based additive. *Energy & Environmental Science* 16: 4084–4092.

71 Adiraju, V.A.K., Chae, O.B., Robinson, J.R. et al. (2023). Highly soluble lithium nitrate-containing additive for carbonate-based electrolyte in lithium metal batteries. *ACS Energy Letters* 8: 2440–2446.

72 Jiang, Z., Zeng, Z., Yang, C. et al. (2019). Nitrofullerene, a C₆₀-based bifunctional additive with smoothing and protecting effects for stable lithium metal anode. *Nano Letters* 19: 8780–8786.

73 Linert, W., Jameson, R.F., and Taha, A. (1993). Donor numbers of anions in solution: the use of solvatochromic Lewis acid-base indicators. *Journal of the Chemical Society, Dalton Transactions* 3181–3186.

74 Xu, X., Yue, X., Chen, Y. et al. (2023). Li plating regulation on fast-charging graphite anodes by a triglyme-LiNO₃ synergistic electrolyte additive. *Angewandte Chemie International Edition* 62: e202306963.

75 Wen, Z., Fang, W., Wu, X. et al. (2022). High-concentration additive and tri-iodide/iodide redox couple stabilize lithium metal anode and rejuvenate the

inactive Lithium in carbonate-based electrolyte. *Advanced Functional Materials* 32: 2204768.

76 Yan, C., Yao, Y.X., Chen, X. et al. (2018). Lithium nitrate solvation chemistry in carbonate electrolyte sustains high-voltage lithium metal batteries. *Angewandte Chemie International Edition* 57: 14055–14059.

77 Chen, W., Hu, Y., Lv, W. et al. (2019). Lithiophilic montmorillonite serves as lithium ion reservoir to facilitate uniform lithium deposition. *Nature Communications* 10: 4973.

78 Gao, Y., Wu, G., Fang, W. et al. (2024). Transesterification induced multifunctional additives enable high-performance lithium metal batteries. *Angewandte Chemie International Edition* 63: e202403668.

79 Jin, Z., Liu, Y., Xu, H. et al. (2024). Intrinsic solubilization of lithium nitrate in ester electrolyte by multivalent low-entropy-penalty design for stable lithium-metal batteries. *Angewandte Chemie International Edition* 63: e202318197.

80 Fu, L., Wang, X., Chen, Z. et al. (2022). Insights on “nitrate salt” in lithium anode for stabilized solid electrolyte interphase. *Carbon Energy* 4: 12–20.

81 Wang, F., Wen, Z., Zheng, Z. et al. (2023). Memory effect of MgAl layered double hydroxides promotes LiNO_3 dissolution for stable lithium metal anode. *Advanced Energy Materials* 13: 2203830.

82 Wright, P.V. (1998). Polymer electrolytes – the early days. *Electrochimica Acta* 43: 1137–1143.

83 Liu, Q., Peng, B., Shen, M. et al. (2014). Polymer chain diffusion and Li^+ hopping of poly(ethylene oxide)/ LiAsF_6 crystalline polymer electrolytes as studied by solid state NMR and ac impedance. *Solid State Ionics* 255: 74–79.

84 Liu, Z., Zhang, S., Zhou, Q. et al. (2023). Insights into quasi solid-state polymer electrolyte: the influence of succinonitrile on polyvinylene carbonate electrolyte in view of electrochemical applications. *Battery Energy* 2: 20220049.

85 Nguyen, H.L., Luu, V.T., Nguyen, M.C. et al. (2022). Nb/Al co-doped $\text{Li}_7\text{La}_3\text{Zr}_2\text{O}_{12}$ composite solid electrolyte for high-performance all-solid-state batteries. *Advanced Functional Materials* 32: 2207874.

86 Wang, H., Sun, Y., Liu, Q. et al. (2022). An asymmetric bilayer polymer-ceramic solid electrolyte for high-performance sodium metal batteries. *Journal of Energy Chemistry* 74: 18–25.

87 He, Y., Liu, N., and Kohl, P.A. (2020). High conductivity, lithium ion conducting polymer electrolyte based on hydrocarbon backbone with pendent carbonate. *Journal of the Electrochemical Society* 167: 100517.

88 Wang, S., Sun, Q., Zhang, Q. et al. (2023). Li-ion transfer mechanism of ambient-temperature solid polymer electrolyte toward lithium metal battery. *Advanced Energy Materials* 13: 2204036.

89 Bao, D., Tao, Y., Zhong, Y. et al. (2023). High-performance dual-salt plastic crystal electrolyte enabled by succinonitrile-regulated porous polymer host. *Advanced Functional Materials* 33: 2213211.

90 Qiu, G., Shi, Y., and Huang, B. (2022). A highly ionic conductive succinonitrile-based composite solid electrolyte for lithium metal batteries. *Nano Research* 15: 5153–5160.

91 Ren, Z., Li, J., Gong, Y. et al. (2022). Insight into the integration way of ceramic solid-state electrolyte fillers in the composite electrolyte for high performance solid-state lithium metal battery. *Energy Storage Materials* 51: 130–138.

92 Lee, M.J., Han, J., Lee, K. et al. (2022). Elastomeric electrolytes for high-energy solid-state lithium batteries. *Nature* 601: 217–222.

93 Wang, L., He, Y., and Xin, H.L. (2023). Transition from Vogel-Fulcher-Tamman to Arrhenius ion-conducting behavior in poly(ethyl acrylate)-based solid polymer electrolytes via succinonitrile plasticizer addition. *Journal of the Electrochemical Society* 170: 090525.

94 Hu, Y., Li, L., Tu, H. et al. (2022). Janus electrolyte with modified Li⁺ solvation for high-performance solid-state lithium batteries. *Advanced Functional Materials* 32: 2203336.

95 Tong, Z., Wang, S.-B., Fang, M.-H. et al. (2021). Na–CO₂ battery with NASICON-structured solid-state electrolyte. *Nano Energy* 85: 105972.

96 Jiang, T., He, P., Wang, G. et al. (2020). Solvent-free synthesis of thin, flexible, nonflammable garnet-based composite solid electrolyte for all-solid-state lithium batteries. *Advanced Energy Materials* 10: 1903376.

97 Fan, L.Z., Hu, Y.S., Bhattacharyya, A.J. et al. (2007). Succinonitrile as a versatile additive for polymer electrolytes. *Advanced Functional Materials* 17: 2800–2807.

98 Reber, D., Borodin, O., Becker, M. et al. (2022). Water/ionic liquid/succinonitrile hybrid electrolytes for aqueous batteries. *Advanced Functional Materials* 32: 2112138.

99 Zhang, D., Liu, Y., Sun, Z. et al. (2023). Eutectic-based polymer electrolyte with the enhanced lithium salt dissociation for high-performance lithium metal batteries. *Angewandte Chemie International Edition* 62: e202310006.

100 Fu, F., Liu, Y., Sun, C. et al. (2022). Unveiling and alleviating chemical “crosstalk” of succinonitrile molecules in hierarchical electrolyte for high-voltage solid-state lithium metal batteries. *Energy & Environmental Materials* 6: e12367.

101 Zhang, J., Wu, H., Du, X. et al. (2022). Smart deep eutectic electrolyte enabling thermally induced shutdown toward high-safety lithium metal batteries. *Advanced Energy Materials* 13: 2202529.

102 Wang, A., Geng, S., Zhao, Z. et al. (2022). In situ cross-linked plastic crystal electrolytes for wide-temperature and high-energy-density lithium metal batteries. *Advanced Functional Materials* 32: 2201861.

103 Lee, S.H., Hwang, J.Y., Park, S.J. et al. (2019). Adiponitrile (C₆H₈N₂): a new bi-functional additive for high-performance Li-metal batteries. *Advanced Functional Materials* 29: 1902496.

104 Chen, S., Zhang, J., Nie, L. et al. (2020). All-solid-state batteries with a limited lithium metal anode at room temperature using a garnet-based electrolyte. *Advanced Materials* 33: 2002325.

105 Liu, Q., Zhou, D., Shanmukaraj, D. et al. (2020). Self-healing Janus interfaces for high-performance LAGP-based lithium metal batteries. *ACS Energy Letters* 5: 1456–1464.

106 Liu, H., Xin, Z., Cao, B. et al. (2023). Polyhydroxylated organic molecular additives for durable aqueous zinc battery. *Advanced Functional Materials* 34: 2309840.

107 Yang, W., Du, X., Zhao, J. et al. (2020). Hydrated eutectic electrolytes with ligand-oriented solvation shells for long-cycling zinc-organic batteries. *Joule* 4: 1557–1574.

108 Yang, Y., Wang, J., Du, X. et al. (2023). Cation co-intercalation with anions: the origin of low capacities of graphite cathodes in multivalent electrolytes. *Journal of the American Chemical Society* 145: 12093–12104.

109 Song, H., Xue, S., Chen, S. et al. (2022). Polymeric wetting matrix for a stable interface between solid-state electrolytes and Li metal anode. *Chinese Journal of Structural Chemistry* 41: 48–69.

110 Li, S., Chen, Y.-M., Liang, W. et al. (2018). A superionic conductive, electro-chemically stable dual-salt polymer electrolyte. *Joule* 2: 1838–1856.

111 Hu, Z., Xian, F., Guo, Z. et al. (2020). Nonflammable nitrile deep eutectic electrolyte enables high-voltage lithium metal batteries. *Chemistry of Materials* 32: 3405–3413.

112 Wu, H., Tang, B., Du, X. et al. (2020). LiDFOB initiated in situ polymerization of novel eutectic solution enables room-temperature solid lithium metal batteries. *Advanced Science* 7: 2003370.

113 Moon, H., Jung, G.Y., Lee, J.E. et al. (2023). Starving free solvents: toward immiscible binary liquid electrolytes for Li-metal full cells. *Advanced Functional Materials* 33: 2302543.

114 Zhang, X., Fu, C., Cheng, S. et al. (2023). Novel PEO-based composite electrolyte for low-temperature all-solid-state lithium metal batteries enabled by interfacial cation-assistance. *Energy Storage Materials* 56: 121–131.

115 Kim, B., Yang, S.H., Seo, J.H. et al. (2023). Inducing an amorphous phase in polymer plastic crystal electrolyte for effective ion transportation in lithium metal batteries. *Advanced Functional Materials* 34: 2310957.

116 Yang, Y.N., Jiang, F.L., Li, Y.Q. et al. (2021). A surface coordination interphase stabilizes a solid-state battery. *Angewandte Chemie International Edition* 60: 24162–24170.

117 Zhang, S.S. (2006). A review on electrolyte additives for lithium-ion batteries. *Journal of Power Sources* 162: 1379–1394.

118 Li, L., Liu, J., Li, L. et al. (2024). Pentafluorophenyl diethoxy phosphate: an electrolyte additive for high-voltage cathodes of lithium-ion batteries. *Journal of Energy Storage* 87: 111364.

119 Shi, P., Zheng, H., Liang, X. et al. (2018). A highly concentrated phosphate-based electrolyte for high-safety rechargeable lithium batteries. *Chemical Communications* 54: 4453–4456.

120 Wang, J., Yamada, Y., Sodeyama, K. et al. (2017). Fire-extinguishing organic electrolytes for safe batteries. *Nature Energy* 3: 22–29.

121 Zeng, Z., Murugesan, V., Han, K.S. et al. (2018). Non-flammable electrolytes with high salt-to-solvent ratios for Li-ion and Li-metal batteries. *Nature Energy* 3: 674–681.

122 Chen, S., Zheng, J., Yu, L. et al. (2018). High-efficiency lithium metal batteries with fire-retardant electrolytes. *Joule* 2: 1548–1558.

123 Wang, X.F., He, W.J., Xue, H.L. et al. (2022). A nonflammable phosphate-based localized high-concentration electrolyte for safe and high-voltage lithium metal batteries. *Sustainable Energy & Fuels* 6: 1281–1288.

124 Jiang, L., Cheng, Y., Wang, S. et al. (2023). A nonflammable diethyl ethylphosphonate-based electrolyte improved by synergistic effect of lithium difluoro(oxalato)borate and fluoroethylene carbonate. *Journal of Power Sources* 570: 233051.

125 Wang, X.M., Yasukawa, E., and Kasuya, S. (2001). Nonflammable trimethyl phosphate solvent-containing electrolytes for lithium-ion batteries – I. Fundamental properties. *Journal of the Electrochemical Society* 148: A1058–A1065.

126 Li, S., Zhang, S., Chai, S. et al. (2021). Structured solid electrolyte interphase enable reversible Li electrodeposition in flame-retardant phosphate-based electrolyte. *Energy Storage Materials* 42: 628–635.

127 Sun, H., Liu, J., He, J. et al. (2022). Stabilizing the cycling stability of rechargeable lithium metal batteries with tris(hexafluoroisopropyl)phosphate additive. *Science Bulletin* 67: 725–732.

128 Gu, Y., Fang, S., Yang, L. et al. (2021). Tris(2,2,2-trifluoroethyl) phosphate as a cosolvent for a nonflammable electrolyte in lithium-ion batteries. *ACS Applied Energy Materials* 4: 4919–4927.

129 Han, Y.-K., Yoo, J., and Yim, T. (2015). Why is tris(trimethylsilyl) phosphite effective as an additive for high-voltage lithium-ion batteries? *Journal of Materials Chemistry A* 3: 10900–10909.

130 Zhao, J., Liang, Y., Zhang, X. et al. (2020). In situ construction of uniform and robust cathode–electrolyte interphase for Li-rich layered oxides. *Advanced Functional Materials* 31: 2009192.

131 Xu, G., Huang, S., Cui, Z. et al. (2019). Functional additives assisted ester-carbonate electrolyte enables wide temperature operation of a high-voltage (5 V-class) Li-ion battery. *Journal of Power Sources* 416: 29–36.

132 Zhang, T., Yang, J., Wang, H. et al. (2024). A solubility-limited, non-protonic polar small molecule co-solvent reveals additive selection in inorganic zinc salts. *Energy Storage Materials* 65: 103085.

133 Liao, X., Zheng, X., Chen, J. et al. (2016). Tris(trimethylsilyl)phosphate as electrolyte additive for self-discharge suppression of layered nickel cobalt manganese oxide. *Electrochimica Acta* 212: 352–359.

134 Yim, T. and Han, Y.-K. (2017). Tris(trimethylsilyl)phosphite as an efficient electrolyte additive to improve the surface stability of graphite anodes. *ACS Applied Materials & Interfaces* 9: 32851–32858.

135 Gao, Y., Li, W., Ou, B. et al. (2023). A dilute fluorinated phosphate electrolyte enables 4.9 V-class potassium ion full batteries. *Advanced Functional Materials* 33: 2305829.

136 Liu, M., Zeng, Z., Gu, C. et al. (2023). Ethylene carbonate regulated solvation of triethyl phosphate to enable high-conductivity, nonflammable, and graphite compatible electrolyte. *ACS Energy Letters* 9: 136–144.

137 Yayathi, S., Walker, W., Doughty, D. et al. (2016). Energy distributions exhibited during thermal runaway of commercial lithium ion batteries used for human spaceflight applications. *Journal of Power Sources* 329: 197–206.

138 Ma, Y., Qin, B., Du, X. et al. (2022). Delicately tailored ternary phosphate electrolyte promotes ultrastable cycling of $\text{Na}_3\text{V}_2(\text{PO}_4)_2\text{F}_3$ -based sodium metal batteries. *ACS Applied Materials & Interfaces* 14: 17444–17453.

139 Wang, L., Ren, N., Jiang, W. et al. (2024). Tailoring Na^+ solvation environment and electrode-electrolyte interphases with $\text{Sn}(\text{OTf})_2$ additive in non-flammable phosphate electrolytes towards safe and efficient Na-S batteries. *Angewandte Chemie International Edition* 63: e202320060.

140 Xu, M.Q., Li, W.S., Zuo, X.X. et al. (2007). Performance improvement of lithium ion battery using PC as a solvent component and BS as an SEI forming additive. *Journal of Power Sources* 174: 705–710.

141 Xu, M., Li, W., and Lucht, B.L. (2009). Effect of propane sultone on elevated temperature performance of anode and cathode materials in lithium-ion batteries. *Journal of Power Sources* 193: 804–809.

142 Sano, A. and Maruyama, S. (2009). Decreasing the initial irreversible capacity loss by addition of cyclic sulfate as electrolyte additives. *Journal of Power Sources* 192: 714–718.

143 Hall, D.S., Allen, J.P., Glazier, S.L. et al. (2017). The solid-electrolyte interphase formation reactions of ethylene sulfate and its synergistic chemistry with prop-1-ene-1,3-sultone in lithium-ion cells. *Journal of the Electrochemical Society* 164: A3445–A3453.

144 Li, X., Yin, Z., Li, X. et al. (2013). Ethylene sulfate as film formation additive to improve the compatibility of graphite electrode for lithium-ion battery. *Ionics* 20: 795–801.

145 Cheng, H., Ma, Z., Kumar, P. et al. (2024). Non-flammable electrolyte mediated by solvation chemistry toward high-voltage lithium-ion batteries. *ACS Energy Letters* 9: 1604–1616.

146 Liu, X., Zhang, T., Shi, X. et al. (2022). Hierarchical sulfide-rich modification layer on SiO/C anode for low-temperature Li-ion batteries. *Advanced Science* 9: 2104531.

147 Pires, J., Timperman, L., Castets, A. et al. (2015). Role of propane sultone as an additive to improve the performance of a lithium-rich cathode material at a high potential. *RSC Advances* 5: 42088–42094.

148 Xia, J., Aiken, C.P., Ma, L. et al. (2014). Combinations of ethylene sulfite (ES) and vinylene carbonate (VC) as electrolyte additives in $\text{Li}(\text{Ni}_{1/3}\text{Mn}_{1/3}\text{Co}_{1/3})\text{O}_2/\text{graphite}$ pouch cells. *Journal of the Electrochemical Society* 161: A1149–A1157.

149 Pham, T.D., Bin Faheem, A., Kim, J. et al. (2023). Unlocking the potential of lithium metal batteries with a sulfite-based electrolyte. *Advanced Functional Materials* 33: 2305284.

150 Kim, D.Y., Park, I., Shin, Y. et al. (2019). Ni-stabilizing additives for completion of Ni-rich layered cathode systems in lithium-ion batteries: an ab initio study. *Journal of Power Sources* 418: 74–83.

151 Ren, Y., Lai, T., and Manthiram, A. (2023). Reversible sodium–sulfur batteries enabled by a synergistic dual-additive design. *ACS Energy Letters* 8: 2746–2752.

152 Yu, B.T., Qiu, W.H., Li, F.S. et al. (2006). A study on sulfites for lithium-ion battery electrolytes. *Journal of Power Sources* 158: 1373–1378.

153 Li, B., Wang, Y., Tu, W. et al. (2014). Improving cyclic stability of lithium nickel manganese oxide cathode for high voltage lithium ion battery by modifying electrode/electrolyte interface with electrolyte additive. *Electrochimica Acta* 147: 636–642.

154 Zuo, X., Fan, C., Xiao, X. et al. (2012). High-voltage performance of LiCoO₂/graphite batteries with methylene methanedisulfonate as electrolyte additive. *Journal of Power Sources* 219: 94–99.